SCISPACE
formerly Typeset

Open access • Posted Content • DOI:10.1101/2020.07.17.206995

A novel sialic acid-binding adhesin present in multiple species contributes to the pathogenesis of infective endocarditis — Source link

Meztlli O. Gaytán, Anirudh K. Singh, Shireen A. Woodiga, Surina A. Patel ...+10 more authors

Institutions: Nationwide Children's Hospital, Virginia Commonwealth University, Ohio State University, RWTH Aachen University

Published on: 14 Nov 2020 - bioRxiv (Cold Spring Harbor Laboratory)

Topics: Sialic acid binding, Streptococcus oralis and Sialic acid

Related papers:

- A novel sialic acid-binding adhesin present in multiple species contributes to the pathogenesis of Infective endocarditis
- Role of Neuraminidase-Producing Bacteria in Exposing Cryptic Carbohydrate Receptors for Streptococcus gordonii Adherence.
- Structural Basis for Sialoglycan Binding by the Streptococcus sanguinis SrpA Adhesin.
- Significance of sialic acid in Klebsiella pneumoniae K1 capsules
- Adhesins of oral streptococci

Share this paper:

View more about this paper here: https://typeset.io/papers/a-novel-sialic-acid-binding-adhesin-present-in-multiple-4oeq7g9who

bioRxiv preprint doi: https://doi.org/10.1101/2020.07.17.206995; this version posted November 14, 2020. The copyright holder for this preprint (which was not certified by peer review) is the author/funder. All rights reserved. No reuse allowed without permission.

A novel sialic acid-binding adhesin present in multiple species contributes to the pathogenesis of Infective endocarditis

Meztlli O. Gaytán[1], Anirudh K. Singh[1#], Shireen A. Woodiga[1], Surina A. Patel, Seon-Sook An[2], Arturo Vera-Ponce de León[3], Sean McGrath[4], Anthony R. Miller[4], Jocelyn M. Bush[4], Mark van der Linden[5], Vincent Magrini[4,6], Richard K. Wilson[4,6], Todd Kitten[2] and Samantha J. King[1,6*]

[1]Center for Microbial Pathogenesis, Abigail Wexner Research Institute at Nationwide Children's Hospital, Columbus, Ohio, United States of America.

[2]Philips Institute for Oral Health Research, Virginia Commonwealth University, Richmond, Virginia, United States of America.

[3]Department of Evolution, Ecology and Organismal Biology, The Ohio State University, Columbus, Ohio, United States of America.

[4]Institute for Genomic Medicine, Abigail Wexner Research Institute at Nationwide Children's Hospital, Columbus, Ohio, United States of America.

[5]Institute of Medical Microbiology, German National Reference Center for Streptococci, University Hospital (RWTH), Aachen, Germany.

[6]Department of Pediatrics, The Ohio State University, Columbus, Ohio, United States of America.

[#]Department of Microbiology, All India Institute of Medical Sciences, Bhopal, Madhya Pradesh, India

***** Corresponding Author

Email: Samantha.King@NationwideChildrens.org.

bioRxiv preprint doi: https://doi.org/10.1101/2020.07.17.206995; this version posted November 14, 2020. The copyright holder for this preprint (which was not certified by peer review) is the author/funder. All rights reserved. No reuse allowed without permission.

Abstract

Bacterial binding to platelets is a key step in the development of infective endocarditis (IE). Sialic acid, a common terminal carbohydrate on host glycans, is the major receptor for streptococci on platelets. So far, all defined interactions between streptococci and sialic acid on platelets are mediated by serine rich repeat proteins (SRRPs). However, we identified *Streptococcus oralis* subsp. *oralis* IE-isolates that bind sialic acid but lack SRRPs. In addition to binding sialic acid, some SRRP-negative isolates also bind the cryptic receptor β-1,4-linked galactose through a yet unknown mechanism. Using comparative genomics, we identified a novel sialic acid-binding adhesin, here named AsaA (associated with sialic acid adhesion A), present in IE-isolates lacking SRRPs. We demonstrated that *S. oralis* subsp. *oralis* AsaA is required for binding to platelets in a sialic acid-dependent manner. AsaA comprises a non-repeat region (NRR), consisting of a FIVAR/CBM and two Siglec-like and Unique domains, followed by 31 DUF1542 domains. When recombinantly expressed, Siglec-like and Unique domains competitively inhibited binding of *S. oralis* subsp. *oralis* and directly interacted with sialic acid on platelets. We further demonstrated that AsaA impacts the pathogenesis of *S. oralis* subsp. *oralis* in a rabbit model of IE. Additionally, we found AsaA orthologues in other IE-causing species and demonstrated that the NRR of AsaA from *Gemella haemolysans* blocked binding of *S. oralis* subsp. *oralis,* suggesting that AsaA contributes to the pathogenesis of multiple IE-causing species. Finally, our findings provide evidence that sialic acid is a key factor for bacterial-platelets interactions in a

bioRxiv preprint doi: https://doi.org/10.1101/2020.07.17.206995; this version posted November 14, 2020. The copyright holder for this preprint (which was not certified by peer review) is the author/funder. All rights reserved. No reuse allowed without permission.

broader range of species than previously appreciated, highlighting its potential as a therapeutic target.

Authors summary

Infective endocarditis (IE) is typically a bacterial infection of the heart valves that causes high mortality. Infective endocarditis can affect people with preexisting lesions on their heart valves (Subacute-IE). These lesions contain platelets and other host factors to which bacteria can bind. Growth of bacteria and accumulation of host factors results in heart failure. Therefore, the ability of bacteria to bind platelets is key to the development of IE. Here, we identified a novel bacterial protein, AsaA, which helps bacteria bind to platelets and contributes to the development of disease. Although this virulence factor was characterized in *Streptococcus oralis*, a leading cause of IE, we demonstrated that AsaA is also present in several other IE-causing bacterial species and is likely relevant to their ability to cause disease. We showed that AsaA binds to sialic acid, a terminal sugar present on platelets, thereby demonstrating that sialic acid serves as a receptor for a wider range of IE-causing bacteria than previously appreciated, highlighting its potential as a therapeutic target.

Introduction

The human oral cavity is inhabited by more than 700 bacterial species. *Streptococcus oralis, Streptococcus mitis* and *Gemella haemolysans* are among the early colonizers of

bioRxiv preprint doi: https://doi.org/10.1101/2020.07.17.206995; this version posted November 14, 2020. The copyright holder for this preprint (which was not certified by peer review) is the author/funder. All rights reserved. No reuse allowed without permission.

77 the oral cavity [1, 2]. Although often associated with oral health, oral commensals can
78 also gain access to the bloodstream where some can cause diseases including infective
79 endocarditis (IE) [3-5].
80
81 IE is typically a bacterial infection of the heart valve endothelium. One of the hallmarks
82 of IE is the formation of vegetations, produced by the accumulation of host factors and
83 bacterial proliferation. These vegetations can affect heart valve function and lead to
84 congestive heart failure [6]. IE can have two presentations. Acute IE is sudden and
85 severe; it typically affects previously normal heart valves and is commonly caused by
86 staphylococci. Subacute IE develops gradually and has a more subtle onset, it affects
87 previously damaged heart valves and is commonly caused by oral streptococci,
88 including *S. oralis* [7].
89
90 Although the exact mechanisms that lead to IE development are unknown, it is
91 proposed that bacterial binding to platelets plays a key role in the pathogenesis of this
92 disease [8]. For many streptococcal species, binding to platelets involves the direct
93 interaction of serine rich repeat proteins (SRRPs) with sialic acid, a common terminal
94 carbohydrate [9-15]. SRRPs are large, surface-associated glycoproteins that form fibrils.
95 Members of this adhesin family possess a modular organization, typically including an
96 N-terminal secretion signal that mediates export through an accessory Sec system, and
97 a C-terminal cell-wall anchoring domain. SRRPs also have a non-repeat region (NRR)
98 that mediates adhesion and one or two regions consisting of serine-rich repeats (SRR),

bioRxiv preprint doi: https://doi.org/10.1101/2020.07.17.206995; this version posted November 14, 2020. The copyright holder for this preprint (which was not certified by peer review) is the author/funder. All rights reserved. No reuse allowed without permission.

which are highly glycosylated and proposed to serve as stalks that extend the NRR from the cell surface [16-18].

The NRR of many sialic acid-binding SRRPs consists of a sialic acid binding immunoglobulin-like lectin (Siglec)-like and a Unique domain [9-11, 15, 19, 20]. The Unique domain is proposed to influence the conformation of the Siglec-like domain [21], which directly interacts with sialic acid. The Siglec-like domains of the SRRPs Fap1 (*S. oralis*), GspB (*Streptococcus gordonii*), Hsa (*S. gordonii*) and SrpA (*Streptococcus sanguinis*) contain an arginine residue essential for sialic acid binding within the semi-conserved YTRY motif [9-11, 15, 21, 22].

Studies have demonstrated that the expression of some SRRPs containing Siglec-like and Unique domains is important in IE [15, 23-25]. Since the arginine residue, essential for binding of the SRRP GspB to sialic acid on platelets, contributes to the pathogenesis of *S. gordonii* in a rat model of IE, virulence is attributed to the specific interaction of SRRPs with sialic acid [15]. Hence, the current paradigm establishes that binding to sialic acid on platelets via Siglec-like and Unique domain-containing SRRPs contributes to the pathogenesis of IE.

The SRRP-sialic acid binding mechanism has been described in the IE-causing bacteria *S. gordonii*, *S. sanguinis* and *S. oralis* [9-11, 15, 19, 20]. However, many other bacterial species cause IE through yet undefined mechanisms. Recent work demonstrated that, in addition to binding sialic acid on platelets, *S. oralis* and *S. gordonii* also bind to β-1,4-

bioRxiv preprint doi: https://doi.org/10.1101/2020.07.17.206995; this version posted November 14, 2020. The copyright holder for this preprint (which was not certified by peer review) is the author/funder. All rights reserved. No reuse allowed without permission.

linked galactose, exposed upon sialic acid removal [9, 26]. In *S. oralis,* adhesion to both sialic acid and β-1,4-linked galactose requires the SRRP Fap1 [9]. This novel strategy of binding multiple receptors reveals that streptococcal-platelet interactions are more complex than previously considered.

In this study, we identified *S. oralis* subsp. *oralis* IE-isolates that bind sialic acid and β-1,4-linked galactose but lack SRRPs. We demonstrated that these strains have a novel sialic acid-binding adhesin, here named AsaA (associated with sialic acid adhesion A), that contributes to the colonization of vegetations in an animal model of IE. AsaA orthologues were also found in several other IE-causing bacterial species suggesting this mechanism of adhesion contributes to the pathogenesis of multiple species.

Results

Serine-rich repeat proteins are not essential for adhesion of *S. oralis* subsp. *oralis* to sialic acid

Bacterial binding to platelets is a key step in the development of IE [8]. Many streptococcal species, including *S. oralis* subsp. *oralis,* bind to sialic acid on platelets via an SRRP [9-11, 15, 19, 20]. Here we demonstrated that only two of five *S. oralis* subsp. *oralis* IE-isolates screened encode the sialic acid-binding SRRP Fap1 (Fig 1A). Since previous reports established that Fap1 binds sialic acid, we tested adhesion of the IE-isolates to this carbohydrate by competing binding with a carbohydrate-binding module (CBM) specific for sialic acid (CBM40, [27]). As shown in Fig 1B, adhesion of the five IE-

bioRxiv preprint doi: https://doi.org/10.1101/2020.07.17.206995; this version posted November 14, 2020. The copyright holder for this preprint (which was not certified by peer review) is the author/funder. All rights reserved. No reuse allowed without permission.

isolates tested was significantly reduced by CBM40. This indicates that while sialic acid is a conserved receptor for all strains tested, Fap1 is not essential for binding this carbohydrate.

Isolates that bind sialic acid but lack *fap1* must either encode a distinct SRRP or employ an alternative adhesion mechanism. To address the first possibility, we screened for the presence of the three different *secA2* variants identified in *S. oralis* (Uo5, F0392 and ATCC6249). SecA2 is the ATPase that energizes export of SRRPs and is more highly conserved than members of the SRRP family [28]. The gene encoding SecA2 was only detected in the *fap1*$^{+}$ isolates, suggesting that the *fap1*$^{-}$ isolates lack other SRRPs (S1 Fig). The absence of genes encoding an SRRP and the machinery required for its export were confirmed by genomic sequencing of two *fap1*$^{-}$ isolates. Overall, these data indicate that sialic acid is a conserved receptor for *S. oralis* subsp. *oralis*, but that SRRPs are not essential for binding this carbohydrate. Instead, SRRP^{-} isolates must bind sialic acid through a novel mechanism.

β-1,4-linked galactose can serve as a receptor for some SRRP^{-} *S. oralis* subsp. *oralis* isolates

We previously demonstrated that β-1,4-linked galactose, exposed upon removal of sialic acid by bacterial neuraminidase, serves as an additional receptor for *S. oralis* subsp. *oralis* binding to platelets [9]. Binding to β-1,4-linked galactose was reported to be Fap1 dependent, hence, it was unclear whether the *fap1*$^{-}$ isolates can bind this carbohydrate. In order to address this question, carbohydrates underlying sialic acid were exposed by

bioRxiv preprint doi: https://doi.org/10.1101/2020.07.17.206995; this version posted November 14, 2020. The copyright holder for this preprint (which was not certified by peer review) is the author/funder. All rights reserved. No reuse allowed without permission.

neuraminidase pretreatment and binding to β-1,4-linked galactose tested by determining whether CBMs previously shown to specifically bind this carbohydrate (CBM71-1.2) can competitively inhibit adhesion [29]. As previously reported for other Fap1$^+$ isolates, the two Fap1$^+$ strains included in this study were significantly reduced in adhesion upon neuraminidase treatment and further reduced upon addition of CBM71-1.2 (Fig 2B). This result supports previous data demonstrating that Fap1$^+$ isolates bind both sialic acid and β-1,4-linked galactose [9]. Binding of the *fap1*$^-$ isolates IE1 and IE18 was not reduced by removal of sialic acid, indicating that binding to underlying carbohydrates is as efficient as binding to sialic acid (Fig. 2A). The fact that addition of CBM71-1.2 significantly reduced adhesion of these strains to neuraminidase treated platelets demonstrates that these SRRP$^-$ isolates can bind β-1,4-linked galactose. Unlike IE1 and IE18, binding of the SRRP$^-$ isolate IE12 to neuraminidase treated platelets was not reduced by CBM71-1.2, indicating that this strain binds sialic acid but not β-1,4-linked galactose (Fig 2A). Together, our data demonstrate that SRRPs are not essential for binding to sialic acid and β-1,4-linked galactose. Therefore, SRRP$^-$ strains must use an alternative mechanism to bind these carbohydrates. Furthermore, the differences in carbohydrate binding capabilities displayed by the SRRP$^-$ isolates suggest that distinct adhesins mediate binding to sialic acid and β-1,4-linked galactose.

SRRP$^-$ isolates employ a novel mechanism of adherence that requires a Sortase A-dependent surface protein(s)

To identify the mechanism(s) by which *S. oralis* subsp. *oralis* strains lacking SRRPs bind to carbohydrates on platelets, we first tested the effect of a Sortase A (SrtA) mutant

bioRxiv preprint doi: https://doi.org/10.1101/2020.07.17.206995; this version posted November 14, 2020. The copyright holder for this preprint (which was not certified by peer review) is the author/funder. All rights reserved. No reuse allowed without permission.

on bacterial binding. SrtA mediates covalent attachment of many adhesins to the cell wall of Gram-positive bacteria [30, 31]. Deletion of *srtA* from SRRP$^-$ isolates, IE12 and IE18, significantly reduced bacterial binding to platelets (Fig 3A). Complementation of the *srtA* mutants significantly increased adhesion, confirming that the phenotype observed was due to the mutation introduced. These results indicate that a surface protein(s), attached to the cell wall by SrtA, is required for adhesion. Sialic acid serves as the main receptor for IE12 and IE18 on platelets (Fig 1B). However, IE18 also binds β-1,4-linked galactose exposed upon sialic acid removal (Fig 2A). Adhesion of an IE18 *srtA* mutant to neuraminidase-pretreated platelets was also reduced (Fig 3A). The adhesion phenotype was recovered upon complementation. These results indicate that a SrtA-dependent surface protein(s) is also required for adhesion to β-1,4-linked galactose.

The above experiments established that SRRP$^-$ isolates bind to platelets through a novel mechanism that requires a surface protein(s), anchored by SrtA. To identify putative sialic acid and β-1,4-linked galactose binding adhesins we performed comparative genomic analysis. Since SrtA recognizes surface proteins that possess an LPxTG amino acid motif [32], the comparative analysis was restricted to genes encoding proteins with this motif. Potential sialic acid-binding adhesins were identified as LPxTG-containing proteins encoded by IE12 and IE18, two SRRP$^-$ isolates that bind this carbohydrate, but absent in the SRRP$^+$ strain ATCC10557. Proteins encoded by IE18, but absent in IE12 and ATCC10557, were considered as potential β-1,4-linked galactose binding adhesins. As seen in Fig 3B, four potential adhesins for each

bioRxiv preprint doi: https://doi.org/10.1101/2020.07.17.206995; this version posted November 14, 2020. The copyright holder for this preprint (which was not certified by peer review) is the author/funder. All rights reserved. No reuse allowed without permission.

carbohydrate were identified (S1 Table). However, the distribution of only one potential adhesin for each carbohydrate correlated with the binding phenotypes of the isolates (Fig 3C and S2 Fig). These results support the hypothesis that SRRP$^-$ isolates bind sialic acid and β-1,4-linked galactose through novel mechanisms involving the SrtA-dependent proteins encoded by IE12_1764 and IE18_0557, respectively.

IE18_0557 encodes a Csh-like protein

IE18_0557 was the only gene encoding a putative β-1,4-linked galactose binding adhesin present in all SRRP$^-$ strains that bind this carbohydrate (Fig 3C and S2 Fig). IE18_0557, which is expressed in IE18 (S3 Fig), is predicted to encode a 3097 amino acid protein that shares 76% amino acid identity with *S. gordonii* CshA (Sg_CshA). Sg_CshA is a fibril-forming adhesin involved in autoaggregation and adhesion to extracellular matrix proteins and other bacterial species [33-35]. The NRR of *S. gordonii* CshA consists of three distinct non-repetitive domains: NR1, NR2 and NR3. The NR2 adopts a lectin-like fold, which is characteristic of carbohydrate binding proteins [36]. In addition, the expression of CshA is associated with lactose-sensitive interactions between *S. gordonii* and *Actinomyces naeslundii* [33]. Together, these data suggest that the protein encoded by IE18_0557, which we have named "Csh-like," is involved in binding to β-1,4-linked galactose.

The Csh-like protein encoded by IE18 contains an YSIRK type signal peptide, an NRR and 23 repeats of the CshA-type fibril repeat (Fig 4A). Homology detection and structural prediction using HHpred [37], revealed that the NRR of this protein shares

bioRxiv preprint doi: https://doi.org/10.1101/2020.07.17.206995; this version posted November 14, 2020. The copyright holder for this preprint (which was not certified by peer review) is the author/funder. All rights reserved. No reuse allowed without permission.

structural similarity with the NR2 of *S. gordonii* CshA (PDB: 5L2D_B, [36]), supporting the hypothesis that Csh-like is required for binding to β-1,4-linked galactose. To validate this hypothesis, we generated a *csh-like* mutant. However, when performing adherence assays with the IE18 *csh-like* mutant bacterial numbers added to the assay were inconsistent; after examination with Gram-staining we observed that the mutant was forming aggregates (S4 Fig) that were not disrupted by vortexing and hence interfered with the platelet-binding assays. As an alternative approach, we examined the effect of adding recombinant Csh-like NRR (Csh_NRR) to IE18 adhesion assays. As expected, binding of IE18 to neuraminidase-pretreated platelets was reduced by CBM71-1.2; however, the addition of Csh_NRR did not significantly reduce binding (Fig 4B). Proper folding of the Csh_NRR was confirmed by circular dichroism (CD) spectroscopy (S5 Fig). These results do not support the hypothesis that Csh-like mediates binding of SRRP$^-$ strains to β-1,4-linked galactose.

IE12_1764 encodes a putative sialic acid-binding protein

Through comparative genomics we identified four potential sialic acid-binding adhesins present in IE12 and IE18 (Fig 3B). However, only IE12_1764 (IE18_0535) was absent in Fap1$^+$ strains but present in all SRRP$^-$ strains that bind sialic acid (Fig 3C and S2 Fig). This putative sialic binding adhesin encoded by IE12 and IE18 consists of an N-terminal YSIRK-type secretion signal, followed by an NRR and 31 or 28 DUF1542 domains, respectively. The NRRs of these proteins share 98.72% amino acid identity, suggesting that they both perform the same function. To facilitate data interpretation, further studies were performed only in IE12, which unlike IE18, binds only to sialic acid.

bioRxiv preprint doi: https://doi.org/10.1101/2020.07.17.206995; this version posted November 14, 2020. The copyright holder for this preprint (which was not certified by peer review) is the author/funder. All rights reserved. No reuse allowed without permission.

IE12_1764, which we confirmed is expressed in IE12 (S3 Fig), encodes a 3146 amino acid protein. Homology detection and structural prediction using HHpred [37] revealed that the N-terminal region of the NRR shares structural homology with both a putative CBM (77.74% probability, PDB: 4NUZ) and a FIVAR (found in various architectures) domain (60.11% probability, PDB: 6GV8). FIVAR domains are also found in some characterized adhesins like Ebh and Embp from *Staphylococcus aureus* and *Staphylococcus epidermidis*, respectively, and are involved in binding to fibronectin [38]. The FIVAR/CBM region is followed by two predicted Siglec-like and Unique domains that share structural similarity with similar domains found in the sialic acid-binding SRRPs Hsa (99.38 and 99.26% probability, PDB: 6EFC), SrpA (99.21 and 99.15% probability, PDB: 5KIQ) and GspB (99.06 and 98.97% probability, PDB: 3QC5) (Fig 5A and B); however, most characterized SRRPs have only one Siglec-like and Unique domain [15, 21, 39]. The NRR is followed by 31 DUF1542 domains, which were previously shown to form fibrils when overexpressed [40]. Overall, these data lead to the hypothesis that IE12_1764 encodes a novel sialic acid-binding adhesin, here named AsaA (Associated with sialic acid adhesion).

AsaA is a novel sialic acid-binding adhesin

A non-polar mutation in *asaA* (IE12 Δ*asaA*) significantly reduced binding of IE12 to platelets. Moreover, sialic acid removal by neuraminidase pretreatment did not further reduce adhesion of IE12 Δ*asaA* (Fig 5C), demonstrating that AsaA is required for bacterial binding to platelets in a sialic acid-dependent manner. Our attempts to

bioRxiv preprint doi: https://doi.org/10.1101/2020.07.17.206995; this version posted November 14, 2020. The copyright holder for this preprint (which was not certified by peer review) is the author/funder. All rights reserved. No reuse allowed without permission.

283 complement the *asaA* mutant were unsuccessful, likely due to the high number of
284 repeats; however, a second independent *asaA* mutant was similarly reduced in
285 adhesion (S6 Fig).
286
287 AsaA consists of an NRR followed by 31 DUF1542 domains. In SRRPs, the NRR,
288 specifically the Siglec-like and Unique domain within it, mediates adhesion to sialic acid.
289 To dissect the role of the different AsaA domains in adhesion we constructed isogenic
290 mutants lacking the entire NRR or the Siglec-like and Unique domains. To monitor
291 protein stability and localization a 3xFLAG tag was added to the parental strain (IE12
292 *asaA* WT-3F) used to generate the mutants (IE12 *asaA* ΔNRR-3F and ΔSU-3F).
293 Binding of the WT-3F strain to platelets was reduced as compared to the untagged IE12
294 (S7 Fig). However, the isogenic mutants lacking either the entire NRR or the Siglec-like
295 and Unique domains were significantly reduced in adhesion to platelets as compared to
296 the WT-3F parental strain (Fig 5D). Importantly, we demonstrated that the isogenic
297 mutants are stable and localized on the cell surface (Fig 5E-F). These results indicate
298 that the NRR of AsaA, specifically the Siglec-like and Unique domains, are required for
299 bacterial binding to platelets.
300
301 Next, we demonstrated that the recombinantly expressed NRR (AsaA_NRR)
302 competitively inhibits binding of IE12 to platelets in a dose-dependent manner (Fig 6A).
303 IE12 adhesion was not reduced by glutathione *S*-transferase (GST) alone, indicating
304 that the competitive inhibition of IE12 binding by AsaA_NRR is specific (S8 Fig). We
305 confirmed that this reduction in adhesion is mediated by the predicted Siglec-like and

bioRxiv preprint doi: https://doi.org/10.1101/2020.07.17.206995; this version posted November 14, 2020. The copyright holder for this preprint (which was not certified by peer review) is the author/funder. All rights reserved. No reuse allowed without permission.

306 Unique domains, since addition of a recombinant protein containing only these domains
307 (AsaA_SU_1-2) significantly reduced binding. This reduction in binding is AsaA and
308 sialic acid-dependent (Fig 6B).
309
310 Finally, we addressed whether the reduction in IE12 binding caused by the addition of
311 AsaA_NRR and AsaA_SU_1-2 was due to the direct interaction of these recombinant
312 proteins with sialic acid on platelets. To this end, we examined the ability of platelets
313 pretreated with PBS or neuraminidase to bind to immobilized AsaA_NRR, AsaA_SU_1-
314 2 or GST. While platelets pretreated with PBS bound efficiently to both recombinant
315 proteins, essentially no binding of neuraminidase treated platelets was observed (Fig.
316 6C). Likewise, no binding of platelets to GST was observed. These results establish that
317 AsaA directly binds sialic acid on platelets through the Siglec-like and Unique domains.
318 In summary, our results demonstrate that *S. oralis* subsp. *oralis* AsaA is a novel adhesin
319 that mediates direct binding to sialic acid on platelets.
320
321 **AsaA contributes to the colonization of vegetations by *S. oralis* IE12 in a rabbit**
322 **model of IE**
323 Since binding to sialic acid on platelets is a key step in the development of IE, the
324 impact of AsaA on the virulence of IE12 was evaluated *in vivo*, using a rabbit model of
325 IE [41]. To that end, the IE12 *asaA* mutant and a chloramphenicol-resistant derivative of
326 IE12 (IE12 Cm^r) were co-inoculated into rabbits in which aortic valve damage was
327 induced by catheterization. The following day, rabbits were euthanized and vegetations
328 in or near the aortic valves were removed. The mean colony-forming units (CFUs)

bioRxiv preprint doi: https://doi.org/10.1101/2020.07.17.206995; this version posted November 14, 2020. The copyright holder for this preprint (which was not certified by peer review) is the author/funder. All rights reserved. No reuse allowed without permission.

329 recovered for the *asaA* mutant were significantly lower than those recovered for IE12
330 Cm^r ($1.06x10^8$ vs $3.36x10^8$) (Fig 7). These studies demonstrate that *S. oralis* subsp.
331 *oralis* AsaA contributes to the colonization of vegetations and is a potential virulence
332 factor for IE.
333
334 To further investigate the role of AsaA in binding to other host components present on
335 damaged cardiac surfaces [42, 43], we tested the ability of an IE12 *asaA* mutant to bind
336 to immobilized human fibrinogen and fibronectin. While binding to fibrinogen was not
337 significantly affected for the *asaA* mutant, binding to fibronectin was significantly
338 increased (Fig 8). While this may be the result of more efficient exposure of additional
339 adhesins upon removal of AsaA, these results demonstrate that AsaA does not play a
340 role in binding to fibrinogen or fibronectin.
341
342 **AsaA is present in other IE-causing bacterial species**
343 Most studies of bacterial-platelet interactions have focused on a limited number of
344 bacterial species, such as *S. gordonii* and *S. aureus* [44]. However, there are other
345 bacterial species that cause IE through unknown mechanisms. To investigate if AsaA
346 orthologues were present in other IE-causing species, we performed BLAST searches
347 using the full-length amino acid sequence of *S. oralis* subsp. *oralis* AsaA as a query.
348 AsaA orthologues were identified in other IE-causing bacterial species including *S.*
349 *mitis, Staphylococcus pasteuri*, *Granulicatella elegans* and *G. haemolysans* [45-55].
350 Overall, the protein architecture of these AsaA orthologues is similar to that of *S. oralis*
351 AsaA. They all contain a secretion signal, an NRR, DUF1542 repeats and a cell-wall

bioRxiv preprint doi: https://doi.org/10.1101/2020.07.17.206995; this version posted November 14, 2020. The copyright holder for this preprint (which was not certified by peer review) is the author/funder. All rights reserved. No reuse allowed without permission.

anchoring motif. The NRR of *S. oralis* AsaA consists of a predicted FIVAR/CBM domain followed by two Siglec-like and Unique domains. The same domains were predicted in the AsaA orthologues in *G. haemolysans* M341, *S. pasteuri* 915_SPAS and *G. elegans* ATCC700633, although in the latter the N-terminal region of the NRR only shares structural homology with the FIVAR domain. Notably, we identified three Siglec-like and Unique domains in the NRR of the AsaA orthologue in *S. mitis* B6 (Fig 9A).

As a proof of principle that AsaA orthologues can also act as adhesins, we demonstrated that the NRR of AsaA from *G. haemolysans* M341 (Gh_AsaA_NRR), significantly reduced binding of IE12 to platelets. This reduction in binding was AsaA-dependent as adherence of the IE12 *asaA* mutant was not further reduced by the addition of Gh_AsaA_NRR (Fig 9B). These results demonstrate that AsaA from *G. haemolysans* can serve as a sialic acid-binding adhesin. Thus, this novel mechanism is potentially relevant to the pathogenesis of multiple IE-causing bacterial species.

Discussion

Adhesion to host surfaces is a key step in bacterial pathogenesis. As such, bacterial binding to platelets plays an important role in the development of IE [8]. Initial studies in streptococci demonstrated that these interactions are mediated by SRRPs binding to sialic acid on platelets [9-15]. However, we previously demonstrate that the *S. oralis* subsp. *oralis* SRRP, Fap1, also mediates binding to the cryptic receptor β-1,4-linked galactose. This work revealed that these interactions are more complex than previously

bioRxiv preprint doi: https://doi.org/10.1101/2020.07.17.206995; this version posted November 14, 2020. The copyright holder for this preprint (which was not certified by peer review) is the author/funder. All rights reserved. No reuse allowed without permission.

appreciated. Here, we confirm sialic acid and β-1,4-linked galactose as platelet receptors for *S. oralis* subsp. *oralis.* Nevertheless, our data demonstrate that SRRPs are not essential for binding these carbohydrates. Instead, we identified a novel sialic acid-binding adhesin, here named AsaA, which contributes to *S. oralis* subsp. *oralis* colonization of vegetations in an animal model of IE. The identification of AsaA-orthologues in additional IE-causing species and the demonstration that one of these proteins can competitively inhibit adhesion of a sialic acid-binding strain suggest that this novel adhesin contributes to the pathogenesis of multiple bacterial species that cause IE.

Previous reports have shown that binding of streptococci to platelets glycans is mediated by SRRPs [9-15]. Consistent with this, a previous study identified SRRPs in all 19 *S. gordonii* and *S. sanguinis* genomes analyzed [56]. In contrast, our results demonstrated that SRRPs are not present in all *S. oralis* subsp. *oralis* IE-isolates screened. While the requirement of SRRPs to bind platelet glycans may be specific for certain streptococcal species, our results stablish that SRRPs are not essential for binding of *S. oralis* subsp. *oralis* to sialic acid and β-1,4-linked galactose.

S. oralis subsp. *oralis* IE-isolates lacking SRRPs showed different binding dynamics to β-1,4-linked galactose than isolates encoding Fap1. While binding of Fap1-encoding isolates is reduced upon neuraminidase treatment (Fig2B and [9]), that of the SRRP-negative isolates IE1 and IE18 was either unaffected or increased, respectively (Fig 2A). This suggests that isolates lacking SRRPs bind to carbohydrates underlying sialic

bioRxiv preprint doi: https://doi.org/10.1101/2020.07.17.206995; this version posted November 14, 2020. The copyright holder for this preprint (which was not certified by peer review) is the author/funder. All rights reserved. No reuse allowed without permission.

acid with higher affinity than those dependent on Fap1. This novel binding mechanism requires a SrtA-associated protein. Through comparative genomics and gene distribution analysis, we identified a Csh-like protein as a putative *S. oralis* β-1,4-linked galactose-binding protein.

Csh-like proteins are a widespread family of fibril-forming surface proteins found in oral streptococci such as *S. gordonii, S. oralis, S. mitis and S. sanguinis*. These proteins consist of an antigenically variable NRR and a conserved repetitive domain [57, 58]. The Csh-like protein identified in IE18 shares the highest amino acid identity (76%) with CshA from *S. gordonii*, which mediates lactose sensitive interspecies interactions and possesses a binding domain with a lectin-like fold (NR2) [33, 35, 36, 59]. The presence of Csh-like correlated with binding of SRRP-negative IE-isolates to β-1,4-linked galactose; however, we could not confirm a role for Csh-like in binding this carbohydrate. A *csh*-like mutant displayed a marked aggregation phenotype that interfered with binding assays; the reason for this aggregation phenotype is unknown but could be due to changes in cell hydrophobicity or to the exposure of other surface adhesins involved in aggregation. As an alternative approach, we tested the ability of the recombinantly expressed NRR of Csh-like to competitively inhibit binding to β-1,4-linked galactose; however, despite being properly folded, it did not reduce binding significantly. While our data do not support the hypothesis that Csh-like mediates binding of *S. oralis* to β-1,4-linked galactose, we cannot rule out this possibility.

bioRxiv preprint doi: https://doi.org/10.1101/2020.07.17.206995; this version posted November 14, 2020. The copyright holder for this preprint (which was not certified by peer review) is the author/funder. All rights reserved. No reuse allowed without permission.

In this work, we identified a novel sialic acid-binding adhesin, named AsaA, that is present in *S. oralis* subsp. *oralis* IE-isolates lacking SRRPs. An *asaA* mutant was reduced in binding to platelets, indicating that AsaA is required for adhesion. Additionally, we established that binding was sialic acid-dependent as removal of this carbohydrate did not further reduce binding of the mutant. We demonstrated that binding to platelets requires the AsaA Siglec-like and Unique domains, as a deletion mutant lacking these domains was reduced in adhesion. Finally, we established the role of AsaA as an adhesin by demonstrating that the recombinantly expressed NRR, specifically the Siglec-like and Unique domains, competitively inhibited adhesion of *S. oralis* subsp. *oralis* and directly bound to sialic acid on platelets.

In the most extensively studied SRRPs, Fap1, GspB, Hsa and SrpA, sialic acid interactions are mediated by a single Siglec-like domain [9-11, 15, 19-21]. This domain is invariably followed by a Unique domain, proposed to allosterically modulate the conformation of the Siglec-like domain [21]. In these SRRPs, Siglec-like domains have a semi-conserved YTRY motif containing an arginine residue essential for sialic acid binding [9-11, 15, 21, 22]. AsaA contains two Siglec-like and two Unique domains. $AsaA_{Siglec1}$ contains a non-canonical YTRY motif (GTRY), which includes the arginine required for sialic acid binding. However, $AsaA_{Siglec2}$ does not possess a YTRY motif. Two previously characterized SRRPs, FapC and SK1, also possess two Siglec-like and two Unique domains. In FapC, only the first Siglec-like domain has the conserved arginine; however, it is not essential for FapC binding to sialic acid on salivary proteins [39]. In SK1, neither of the Siglec-like domains has a conserved arginine and yet the

bioRxiv preprint doi: https://doi.org/10.1101/2020.07.17.206995; this version posted November 14, 2020. The copyright holder for this preprint (which was not certified by peer review) is the author/funder. All rights reserved. No reuse allowed without permission.

443 protein binds sialic acid. How Siglec-like domains lacking the arginine of the YTRY motif
444 bind sialic acid is unknown; however, a recent study suggests that additional
445 interactions can occur between Siglec-like domains and sialoglycans through three
446 flexible loops [20]. Together, these data suggest that both AsaA Siglec-like domains
447 bind sialic acid. The impact of having two tandem repeats of Siglec-like and Unique
448 domains is also unknown. However, previous studies showed that increasing the
449 number of binding domains can increase affinity [29, 60]. Additionally, the NRR of SK1,
450 containing two Siglec-like and Unique domains, binds a wider variety of sialoglycans
451 than characterized SRRPs containing only one Siglec-like and Unique domain [21].
452 Hence, it is possible that increasing the number of Siglec-like and Unique domains
453 broadens protein selectivity and impacts tropism, by expanding the range of host
454 receptors than can be bound.
455
456 As indicated by their name, FIVAR domains are found in various bacterial proteins.
457 FIVAR domains have been found in some CAZymes (Carbohydrate-active enzymes),
458 and hence they are referred to as putative, yet uncharacterized, CBMs [61-65]. Since
459 these domains share structural homology with heparin binding modules, it was
460 suggested that they could bind negatively charged polysaccharides [63]. In agreement
461 with the hypothesis that FIVAR domains bind carbohydrates, this region of AsaA was
462 predicted to share structural homology with a putative CBM present in an endo-β-*N*-
463 acetylglucosaminidase (EndoS) from *Streptococcus pyogenes* (PDB: 4NUZ) [66]. The
464 putative CBM from EndoS shares structural homology to CBM62, which binds
465 galactose-containing polysaccharides [66]. Although the ligands of the EndoS CBM

bioRxiv preprint doi: https://doi.org/10.1101/2020.07.17.206995; this version posted November 14, 2020. The copyright holder for this preprint (which was not certified by peer review) is the author/funder. All rights reserved. No reuse allowed without permission.

466 remain unknown, nuclear magnetic resonance analysis showed potential low affinity
467 binding to D-galactose [67]. These data suggest that, like Fap1, AsaA is involved in
468 binding β-1,4-linked galactose exposed by neuraminidase cleavage of sialic acid [9].
469 However, an *asaA* mutant did not reduce binding of IE18 to neuraminidase pretreated
470 platelets (S9 Fig). Additionally, the fact that neuraminidase pretreated platelets, which
471 have exposed β-1,4-linked galactose, did not bind to the immobilized AsaA_NRR rules
472 out a role for AsaA in binding to β-1,4-linked galactose. Although the role of the FIVAR
473 domain is unclear, in our deletion mutants (Fig 5D) and platelet binding assay (Fig 6D)
474 the presence of this domain tends to increase platelet binding. These data did not reach
475 significance ($P \leq 0.250$ and 0.09, respectively), therefore further studies are required to
476 define the role of the FIVAR domain in AsaA.
477
478 FIVAR domains are also found in adhesive molecules such as Ebh from *S. aureus* and
479 Embp from *S. epidermidis* [38, 68-70], which possess more than 40 FIVAR domains.
480 Tandem FIVAR domains directly interact with the glycoprotein fibronectin [38]. However,
481 we demonstrated that AsaA, which has only one FIVAR domain, is not involved in
482 binding to fibronectin; whether this activity requires the presence of several FIVAR
483 domains remains to be determined.
484
485 According to Lin *et al*, DUF1542 is the most repeated domain in streptococci [71].
486 Although Ebh and Embp consist mainly of FIVAR domains, these adhesins also
487 possess four and seven DUF1542 domains, respectively [38, 68]. Additionally, *S.*
488 *aureus* SasC, *Lactobacillus rhamnosus* MabA and *S. pyogenes* Epf possess 17, 26 and

bioRxiv preprint doi: https://doi.org/10.1101/2020.07.17.206995; this version posted November 14, 2020. The copyright holder for this preprint (which was not certified by peer review) is the author/funder. All rights reserved. No reuse allowed without permission.

18 DUF1542 domains, respectively [40, 72, 73]. Previous studies demonstrated that the DUF1542 domains present in SasC and Epf are not involved in adhesion, cell aggregation or biofilm enhancement [40, 72]. Instead, these domains form long, flexible, thin, fiber-like structures when overexpressed [40]. Thus, it is likely that AsaA forms a surface fibril.

A protein architecture similar to that of AsaA, consisting of an NRR followed by a DUF1542 domain stalk, is also found in Epf, MabA and SasC [40, 72, 73]. However, as observed in the SRRP-family, each adhesin possesses a unique NRR. The NRR of Epf is comprised of two subdomains, one is structurally similar to CBMs and the other adopts a fibronectin type III fold [40]. The structure of the NRRs of MabA and SasC are unknown; however, HHPred searches identified structural similarity between the NRR of MabA and the CBM-like domain of Epf [37, 40]. We propose that AsaA, Epf, SasC and MabA form part of a novel family of bacterial adhesins, here named DRAs (DUF1542-Repeat Adhesins), with a similar protein architecture.

Different NRRs are present in both DRAs and SRRPs, suggesting that these protein families can be a source of intra and interspecies diversity in receptor binding. Horizontal gene transfer between these organisms could lead to replacement of binding domains. The repeat domains in each protein family (Serine-rich and DUF1542) are not involved in adhesion, but are proposed to function as a stalk that helps the adhesive NRR protrude beyond the cell surface [40, 74, 75]. However, these domains are clearly different and may have a distinct impact on the biology of the organism. Serine-rich

bioRxiv preprint doi: https://doi.org/10.1101/2020.07.17.206995; this version posted November 14, 2020. The copyright holder for this preprint (which was not certified by peer review) is the author/funder. All rights reserved. No reuse allowed without permission.

repeats are heavily glycosylated, which is important in biofilm development [76]. Additionally, these glycosylated adhesins require a specialized accessory Sec-System for their export [17]. No accessory Sec-system was found in the AsaA-encoding isolates, additionally, AsaA possess a YSIRK signal peptide that may drive its export through the general Sec-system. These data suggest that AsaA is not glycosylated and its synthesis and export is likely less energetically expensive than that of SRRPs. The expression of SRRPs has also been associated with high cell hydrophobicity [77]; therefore, SRR and DUF1542 domains will likely impact the biology of the organism in ways that are yet to be appreciated. Further experiments, beyond the scope of this study, are underway to establish the role of the repeat domains and their biological implications.

Adhesion is a key bacterial process during to host colonization, and hence it is linked to the virulence potential of bacteria. In streptococci, the expression of SRRPs is important for virulence in animal models of IE [15, 23-25, 78]. This phenotype is attributed to the ability of SRRPs to bind sialic acid on platelets [15]. Likewise, our data indicate that *S. oralis* AsaA is important for the colonization of vegetations in an *in vivo* model of IE. We observed a 3-fold reduction in the number of mutant bacteria recovered from the vegetations. Although a direct comparison with other *in vivo* studies is impractical due to variations in the models employed, this result is consistent with previous observations [14, 25, 78]. Additionally, the reduction in *asaA* mutant bacteria recovered is likely associated with the inability of the *asaA* mutant to bind sialic acid on platelets. In addition to platelets, other host factors such as fibrinogen and fibronectin are present on

bioRxiv preprint doi: https://doi.org/10.1101/2020.07.17.206995; this version posted November 14, 2020. The copyright holder for this preprint (which was not certified by peer review) is the author/funder. All rights reserved. No reuse allowed without permission.

535 the damaged valve surface and contribute to initial bacterial binding [42, 43]. An *asaA*
536 mutant was increased in binding to fibronectin, likely due to the absence of AsaA
537 exposing other adhesins. This increased binding to other host factors may have partially
538 compensated for the loss of AsaA *in vivo.* Our data demonstrate that AsaA contributes
539 to the colonization of vegetations; however, more studies will be required to determine
540 the impact on the course of disease.
541
542 We identified AsaA orthologues in other IE-causing species including *G. haemolysans,*
543 *G. elegans, S. pasteuri* and *S. mitis* [45, 47, 48, 52, 53]. A previous study identified
544 DUF1542-containing proteins in five *S. mitis* strains [79]. Although these were not
545 characterized, we used Pfam and HHpred to determine that these proteins are AsaA
546 orthologues, possessing Siglec-like and Unique domains in the N-terminal region. The
547 overall architecture of these proteins is similar, however, some display differences in the
548 NRR domains and the number of DUF1542 repeats. The AsaA orthologue in *S. mitis* B6
549 lacks the FIVAR/CBM domain, suggesting it is dispensable for protein function. Of note,
550 the *S. mitis* AsaA orthologue contains three distinct Siglec-like and Unique domains in
551 the NRR; to our knowledge, this is the first report of a streptococcal adhesin predicted to
552 contain three such domains. These differences will likely impact the binding affinity and
553 selectivity as discussed above.
554
555 The ability of the *G. haemolysans* AsaA orthologue (Gh_AsaA) to act as an adhesin
556 was demonstrated by the reduction of *S. oralis* adhesion in the presence of the
557 recombinantly expressed Gh_AsaA_NRR. The 40% reduction in binding to platelets

bioRxiv preprint doi: https://doi.org/10.1101/2020.07.17.206995; this version posted November 14, 2020. The copyright holder for this preprint (which was not certified by peer review) is the author/funder. All rights reserved. No reuse allowed without permission.

was less than that observed in the presence of So_AsaA_NRR, the recombinantly expressed NRR of *S. oralis* AsaA. This result could be explained by variation in binding specificity or affinity derived from differences in the amino acid sequence. These results suggest the novel sialic acid-binding adhesin AsaA is a virulence factor important for the pathogenesis of multiple bacterial species that cause IE.

In summary, this study identified a novel sialic acid-binding adhesin that contributes to the virulence of *S. oralis* subsp. *oralis*. AsaA is broadly distributed and likely relevant to the pathogenesis of multiple IE-causing species. We propose that AsaA forms part of a novel family of bacterial adhesins that employ DUF1542 repeats to extend different NRRs beyond the cell surface. The NRRs, which determine the receptors bound, are shared with at least some of those found in SRRPs. However, since the repeat regions of these two families of bacterial adhesins are different, we hypothesize that they will differentially impact traits such as hydrophobicity and biofilm formation. Finally, our work demonstrates that sialic acid is a more broadly conserved receptor than previously appreciated, highlighting the importance of this bacterial adhesion mechanism in the biology of these organisms.

Materials and methods

Bacterial strains and culture media

All bacterial strains and plasmids used in this study are listed in Table 1. The five *S. oralis* strains included in the study, confirmed as subsp. *oralis* by MLSA, were selected

bioRxiv preprint doi: https://doi.org/10.1101/2020.07.17.206995; this version posted November 14, 2020. The copyright holder for this preprint (which was not certified by peer review) is the author/funder. All rights reserved. No reuse allowed without permission.

581 from a group of eight isolates for their ability to bind efficiently and reproducibly to
582 platelets in a sialic-acid dependent manner. *S. oralis* subsp. *oralis* was grown on tryptic
583 soy agar plates (TSA) supplemented with 5% sheep blood (Becton, Dickinson and Co.)
584 at 37°C in a 5% CO_2 atmosphere for 16 h. Liquid cultures were grown statically at 37°C
585 in Todd-Hewitt broth (Becton, Dickinson and Co.) supplemented with 0.2% (w/v) yeast
586 extract (Becton, Dickinson and Co.) (THY). *Escherichia coli* strains were grown
587 aerobically in lysogeny broth (LB) at 37°C with constant shaking at 250 rpm. When
588 necessary, *S. oralis* subsp. *oralis* growth media was supplemented with the appropriate
589 antibiotics at the following concentrations: 200 µg/mL spectinomycin, 500 µg/mL
590 kanamycin or 2.5 µg/mL chloramphenicol. *E. coli* growth media was supplemented with
591 100 µg/mL ampicillin, 50 µg/mL spectinomycin, 50 µg/mL kanamycin or 30 µg/mL
592 chloramphenicol when required.
593

Table 1. Strains and plasmids

Strain or plasmid	Characteristics or genotype[a]	Source or reference
Strain		
Streptococcus oralis subsp. *oralis*		
SN16516 (IE1)	Infective endocarditis isolate	GNRCS[b]
SN18825 (IE4)	Infective endocarditis isolate	GNRCS
SN59433 (IE15)	Infective endocarditis isolate	GNRCS
SN51445 (IE12)	Infective endocarditis isolate	GNRCS
IE12 Δ*srtA*	*srtA::aad9* Spc^r	This study
IE12 Δ*srtA*/pABG5	*srtA::aad9* Spc^r transformed with the empty pABG5 vector.	This study
IE12 Δ*srtA*/pABG5-*srtA*	*srtA::aad9* Spc^r transformed with pABG5 expressing *srtA*	This study
IE12 Δ*asaA*	*asaA*::kan Kan^r	This study
IE12 *asaA*_NRR::Cm	*asaA*_NRR::*cat* Cm^r	This study
IE12 *asaA* WT-3F	*asaA-3xFLAG* Spc^r	This study
IE12 *asaA* ΔNRR-3F	*asaA* ΔNRR-*3xFLAG* Spc^r	This study
IE12 *asaA* ΔSU-3F	*asaA* ΔSU-*3xFLAG* Spc^r	This study
IE12 Cm^r	IR^c::*cat* Cm^r	This study
SN64428 (IE18)	Infective endocarditis isolate	GNRCS
IE18 Δ*srtA*	*srtA::aad9* Spc^r	This study
IE18 Δ*asaA*	*asaA*::kan Kan^r	This study
IE18 Δ*srtA*/pABG5	*srtA::aad9* Spc^r transformed with the empty pABG5 vector.	This study
IE18 Δ*srtA*/pABG5-*srtA*	*srtA::aad9* Spc^r transformed with pABG5 expressing *srtA*	This study
IE18 Δ*csh*-like	*csh*-like*::aad9* Spc^r	This study
Uo5	Highly penicillin- and cephalosporin-resistant strains isolated from the nasal cavity of a healthy individual	[80]
Streptococcus oralis subsp. *dentisani* F0392	Originally identified as Streptococcus mitis, isolated from the human oral cavity	BEI Resources[d]

bioRxiv preprint doi: https://doi.org/10.1101/2020.07.17.206995; this version posted November 14, 2020. The copyright holder for this preprint (which was not certified by peer review) is the author/funder. All rights reserved. No reuse allowed without permission.

Streptococcus oralis genomosubspecies 1 ATCC 6249	Human blood from a patient with septicemia and endocarditis	ATCC
Gemella haemolysans M341	Strain M341, HM-239. Isolated from the human oral cavity	BEI Resources[d]
Escherichia coli		
Stellar	Cloning host	Takara
BL21 (DE3)	*fhuA2* [*lon*] *ompT gal* (λ DE3) [*dcm*] Δ*hsdS*	New England Biolabs
Plasmids		
pDrive	Cloning vector, Amp^r Kan^r	Qiagen
pDriveΔ*srtA*	pDriveΔ*srtA*::*aad9* Spc^r Amp^r Kan^r	This study
pJET1.2/Blunt	Cloning vector, Amp^r	Thermo Fisher Scientifi
pJETΔ*asaA*	pJETΔ*asaA*::*kan/rpsL*$^+$ *rpsL*(K56T) Kan^r Amp^r	This study
pJET*asaA*_NRR::Cm[e]	pJET*asaA* NRR::*cat* Cm^r Amp^r	This study
pJET*asaA*WT-3F	pJET*aad9_asaA-3xFLAG* Spc^r Amp^r	This study
pJET*asaA*ΔNRR-3F[e]	pJET*aad9_asaA*ΔNRR-*3xFLAG* Spc^r Amp^r	This study
pJET*asaA*ΔSU-3F	pJET*aad9_asaA*ΔSU-*3xFLAG* Spc^r Amp^r	This study
pJETΔ*csh*	pJETΔ*csh*::*aad9* Spc^r Amp^r	This study
pJETIR::Cm	pJETIR::*cat* Cm^r Amp^r	This study
pABG5	Streptococcal shuttle vector, Cm^r Kan^r	[81]
pABG5-*srtA*	pABG5.1 encoding the *srtA* gene	This study
pOPINF	T7-based expression vector, Amp^r	Novagen
pOPINFSpCBM40	pOPINF, encoding *S. pneumoniae* CBM40, Amp^r	[39]
pOPINFSpCBM71 1.2	pOPINF, encoding *S. pneumoniae* CBM71 1.2, Amp^r	[29]
pOPINF_18_Csh_NRR[e]	pOPINF, encoding the NRR of Csh-like from *S. oralis* IE18, Amp^r	This study
pGEX-5X-3	Expression vector, Amp^r	GE Biosciences
pGEX_So_AsaA_NRR[e]	pGEX containing the NRR of AsaA from *S. oralis* IE12, Amp^r	This study
pGEX_So_AsaA_SU1-2	pGEX containing the both Siglec-like and Unique domains of AsaA from *S. oralis* IE12, Amp^r	This study
pGEX_Gh_AsaA_NRR[e]	pGEX containing the NRR of AsaA from *G. haemolysans*, Amp^r	This study

[a]Spc^r, spectinomycin resistant; Kan^r, kanamycin resistant; Cm^r, chloramphenicol resistant; Amp^r, ampicillin resistant.
[b]GNRCS, German National Reference Center for Streptococci.
[c]IR, intergenic region.
[d]This strain was obtained through BEI Resources, NIAID, NIH as part of the Human Microbiome Project.
[e]Non-repeat region

For *in vivo* studies, bacteria were grown overnight at 37°C in brain heart infusion (BHI) broth under microaerobic conditions (6% O_2, 7% H_2, 7% CO_2 and 80% N_2) created with a programmable Anoxomat Mark II jar-filling system (AIG, Inc.); then diluted 10-fold into fresh, pre-warmed BHI and incubated statically at 37°C.

Multilocus sequence analysis (MLSA)

S. oralis subsp. *oralis* isolates were identified using a previously published MLSA scheme [82]. Concatenated sequences of seven housekeeping genes were added to M. Kilian's database of concatenated sequences from mitis group isolates. The species

bioRxiv preprint doi: https://doi.org/10.1101/2020.07.17.206995; this version posted November 14, 2020. The copyright holder for this preprint (which was not certified by peer review) is the author/funder. All rights reserved. No reuse allowed without permission.

609 was confirmed and subspecies assigned using MEGA (version 6.06) software as
610 previously described [83, 84].
611
612 **Genomic DNA isolation and sequencing**
613 Genomic DNA (gDNA) was isolated as previously described [85] with slight
614 modifications. Briefly, cells were grown in THY to an optical density at 600 nm (OD_{600})
615 of 0.6 and harvested by centrifugation. The cell pellet was incubated at 37°C with 150 U
616 of mutanolysin (Sigma) followed by treatment with RNAse A/N1 (100 µg/mL, Thermo
617 Scientific), Proteinase K (100 µg/mL) and N-lauryl sarcosine (final concentration 1.5%).
618 Two Phenol:Chloroform:Isoamyl alcohol (25:24:1) extractions were performed followed
619 by two extractions with Chloroform. DNA was precipitated with isopropanol and washed
620 with cold 70% ethanol. Finally, samples that were sequenced by PacBio were
621 processed in accordance with the Guidelines for Using a Salt:Chloroform Wash to
622 Clean Up gDNA (Pacific Biosciences).
623
624 gDNA from *S. oralis* subsp. *oralis* strains IE12 and IE18 was sheared to 10 kb with the
625 Diagenode Megaruptor 2 converted into a SMRTbell library (Pacific Biosciences) using
626 the SMRTbell express template preparation standard protocol. A total of 2-3.5 µg of the
627 recovered library was concentrated with 0.6X AMPure PB carboxylated paramagnetic
628 beads (Pacific Biosciences). The libraries were prepared for sequencing with Sequel
629 binding kit 3.0 (Pacific Biosciences) at a 3 pM final loading concentration. Each purified
630 library complex was sequenced on one 1Mv2LR SMRT cell with a 6 h pre-extension
631 and 20 h movie time using diffusion loading. Raw sequence data was processed in

bioRxiv preprint doi: https://doi.org/10.1101/2020.07.17.206995; this version posted November 14, 2020. The copyright holder for this preprint (which was not certified by peer review) is the author/funder. All rights reserved. No reuse allowed without permission.

SMRT Link with the "Circular Consensus Sequencing" application to produce >Q20 consensus reads.

S. oralis subsp. *oralis* strain ATCC10557 was sequenced and assembled by the University of Washington PacBio Sequencing Services.

Genome assembly and annotation

All >Q20 consensus reads from the IE12 and IE18 genomes were assembled using Canu v 1.8 assembler with the following parameters genomeSize=1.9m maxThreads=10 maxMemory=20g [86]. BBmap aligner from the BBTools package (https://jgi.doe.gov/data-and-tools/bbtools/) was used to calculate the general assembly statistics (contig length, coverage and GC content) by re-aligning all reads to the corresponding assembly. The assemblies resulted in a circular contig (2,113,732 bp, 407.25x coverage and 40.97% GC content) and two non-circular contigs (14,198 bp 745.15x coverage and 42.6% GC content; 2,092,871 bp, 726.19x coverage and 40.94% GC content) for the IE12 and IE18 genomes, respectively. For both genomes, completeness was estimated as 100% by the BUSCO 3.2.0 pipeline using the Firmicutes group orthologue database with translations of predicted open reading frames in each genome [87]. PROKKA version 1.12 was used for gene prediction and annotation, with SignalP for Gram-positive signal peptides prediction and Infernal for noncoding RNA annotation (--gram +/pos --rfam parameters, respectively) [88-90].

Distribution of *fap1, secA2* and genes encoding potential carbohydrate binding adhesins

bioRxiv preprint doi: https://doi.org/10.1101/2020.07.17.206995; this version posted November 14, 2020. The copyright holder for this preprint (which was not certified by peer review) is the author/funder. All rights reserved. No reuse allowed without permission.

The presence of *fap1* and *secA2* in five *S. oralis* subsp. *oralis* IE-isolates was analyzed by Southern blotting using 2 µg of EcoRV digested gDNA as previously described [26]. Briefly, conserved internal fragments of *fap1* and three different *secA2* genes representing the different variants of this gene identified in *S. oralis,* were amplified using primers Sb.1 - Sb.2 and Sb.3 to Sb.8 (Table 2) and labeled with digoxigenin (DIG) using the PCR DIG probe synthesis kit (Roche Diagnostics). Membranes were hybridized with these probes at 65°C and then washed at 68°C with decreasing concentrations (from 2X to 0.2X) of SSC (150 mM NaCl, 15 mM sodium citrate). Bound probes were detected using the DIG nucleic acid detection kit. As a positive control, all membranes were re-probed with *secA*.

Table 2. Primers used in this study

Target or group	Name	Sequence (5' to 3')	Location (GenBank accession no.)
Southern blot	Sb.1	TTGGTGTTCAAAGTCAGTACC	727082-727102 (CP054135)
	Sb.2	AATTGCGGCAGGGTTGGCTG	726165-726184 (CP054135)
	Sb.3	AGATATCAAACTCGGTCCAG	1526182-1526201 (FR720602.1)
	Sb.4	TAATTCTCTCATCCCAAAGC	1525670-1525689 (FR720602.1)
	Sb.5	TTTACGAATTGATTATCCAG	943735-943754 (CP034442.1)
	Sb.6	TTCTTTGTGATAGTACTCAC	943265-943284 (CP034442.1)
	Sb.7	TGGGACGGATATCAAACTCG	712296-712314 (CP054135)
	Sb.8	ACGACTGGCATAGTGTTTAG	712003-712022 (CP054135)
	Sb.9	TATGTATAAGAAATTGGCAG	497312-497331 (FR720602.1)
	Sb.10	TTGACGTCCTGAACGTCCAC	497794-497813 (FR720602.1)
asaA	A.1	GAGAAGAAAATTTACATCTATA	1753569-1753590 (CP054134)
	A.2	TTTGCATCATCGTTAGTTTGAG	1752329-1752350 (CP054134)
	A.3	AGGTTATGCGCTTTTCAATTCG	1754222-1754243 (CP054134)
	A.4	GAAACAGAGCCTTCTCCACTCG	1752662-1752683 (CP054134)
	A.5	CCATGTGGTTCCATAACGGG	1743777-1743796 (CP054134)
	A.6	TAAATTCCTGGCAAAATTCC	1743057-1743076 (CP054134)
	A.7	TGGCTCGAGTTTTTCAGCAAGATCACTAAGAATCAATTTGATAAGG[a]	1755154-1755176
	A.8	CCAATTTTCGTTTGTTGAACTAGAAGTTACTTTTATTTGTAAA[b]	1754405-1754425
	A.9	AATGTCACTAACCTGCCCCGTCAGTCTGCCATCGATGCTATT[b]	1752160-1752180
	A.10	TGTAGGAGATCTTCTAGAAAGATATTCCACTTGTTTTAGCACTCTC[a]	1751753-1751775

bioRxiv preprint doi: https://doi.org/10.1101/2020.07.17.206995; this version posted November 14, 2020. The copyright holder for this preprint (which was not certified by peer review) is the author/funder. All rights reserved. No reuse allowed without permission.

	A.11	TGTATTCACGAACGAAAATCGGAAGTTACTTTTATTTGTAAA[c]	1754405-1754425
	A.12	GAAAACAATAAACCCTTGCATACACAACTTGCAAAAAGAGCTTA[c]	1754383-1754404
	A.13	TTTATCATCATCATCTTTATAATCTTTATCATCATCATCTTTATAATCTTTATCATCATCATCTTTATAATCTTTGTTTAAAGTTATGAATTCTG	1752181-1752203
	A.14	ATTATAAAGATGATGATGATAAACAGTCTGCCATCGATGCTATTAA	1752158-1752180
	A.15	TCTGAAATTTCTTTTTTTTCAACTTGACTATCCTTCGCGTTACTC	1754047-1754068
	A.16	GAGTAACGCGAAGGATAGTCAAGTTGAAAAAAAAGAAATTTCAGA	1753802-1753824
	A.17	TTGACTATCCTTCGCGTTACTCTGATC	1764047-1754073
	A.18	AGAGTAACGCGAAGGATAGTCAAGATTATAAAGATGATGATGATAA	1754047-1754069
	A.19	GAAGGTCGTGGGATCACACTATTAATGTTTTTAGG[d]	1754165-1754184 (CP054134)
	A.20	GATGCGGCCGCTCGATCATAAAGTTATGAATTCTGATA[d]	1752187-1752206 (CP054134)
	A.21	GAAGGTCGTGGGATCAGTGAAGAAGTTTCAAAAAAC[d]	49801-49821 (GL883584.1)
	A.22	GATGCGGCCGCTCGATCATAAACTTACATATTCTGATA[d]	51851-51870 (GL883584.1)
	A.23	GAAGGTCGTGGGATCACTGAAAATTCGGAGAAA[d]	1753726-1753743 (CP054134)
	A.24	GATGCGGCCGCTCGATCATTTGTTTAAAGTTATGAA[d]	1752181-1752198 (CP054134)
	A.25	TTTAGACAAATAGGCTGAGTG	1754508-1754528 (CP054134)
Csh	C.1	GATGGAGAAGAAGCAAACCCAGG	545471-545493 (JABTEW010000000)
	C.2	AATCATAGCAGCTTGCTGACC	545798-545818 (JABTEW010000000)
	C.3	ATGGGAAAAGAATTATTTAATCC	544382-544401 (JABTEW010000000)
	C.4	ACTTGTAAGTCTTCAACTTCACC	546347-546369 (JABTEW010000000)
	C.5	AGTACAGATCATGCTGATGAAGG	545987-546009 (JABTEW010000000)
	C.6	GTAGCCTCCCTAGTCTCTACTGG	544856-544878 (JABTEW010000000)
	C.7	CTATATCGATGAGGCTCAGC	554287-554306 (JABTEW010000000)
	C.8	CATTCAATCCCGTTGTATCC	554612-554593 (JABTEW010000000)
	C.9	AAGTTCTGTTTCAGGGAGATGAAACAAGCGCT[e]	544505-544519 (JABTEW010000000)
	C.10	CTGGTCTAGAAAGCTCTAAGTAAGGTTAACTTGTAA[e]	546362-546379 (JABTEW010000000)
	C.11	TGATGCTTTATAAATAGCAGG	544129-544149 (JABTEW010000000)
srtA	S.1	TCGGATCCAGAATTCAAGAAGAATAAGCGCAGAAATC[f]	1575983-1576004 (CP054134)
	S.2	CACGAACGAAAATCGTGCTCCGTAGAACAGGTTTACA[c]	1575660-1575681 (CP054134)
	S.3	TCGGATCCAGAATTCGTCGAATTGCCACAGGTGTC[f]	1576448-1576467 (CP054134)
	S.4	CACGAACGAAAATCGATGAGACATTATGCTTCACCTTC[c]	1576029-1576051 (CP054134)
	S.5	ATAAACCCTTGCATAGGCCTTTAATCAACCGTATAG[c]	1575295-1575315 (CP054134)
	S.6	CTTGTCGACGAATTCTCAAGAAACTACCAGCTGTC[f]	1574793-1574812 (CP054134)
	S.7	GGCTGCAGGTGCAGTTGGTGC	1574936-1574956 (CP054134)
	S.8	CAAAGTTCGCAGCAATGTGTTC	1574463-1574484 (CP054134)
	S.9	GACTAGCTCATTGGAACGGCC	1574614-1574634 (CP054134)
	S.10	GAGAGGTCCCTTTCCATGTCTCATAAAAAAACGAA[g]	1575282-1575301 (CP054134)
	S.11	ACCAATACCTTTATCTTAATAACGTTGTCTATAC[g]	1576018-1576037 (CP054134)
IR::*cat*	I.1	TTAAGGCTTTCTTGGGAGATG	124615-124635 (CP054134)
	I.2	TGGTCAACGCCAGCGTATCGG	125808-125828 (CP054134)
	I.3	TACAATTCCCCTTTTACAAGC	125274-125294 (CP054134)
	I.4	TTATCATTAACGTTTAGACCA	125253-125273 (CP054134)
	I.5	TACGATTGGAATTTTAGTCC	123956-123975 (CP054134)
	I.6	ATGTCTGAAAAATTAGTAGA	126267-126286 (CP054134)
IE12_1765	D.1	CAAGCCAATGAAATTGGTGG	1760169-1760188 (CP054134)
	D.2	TAACCAACATACTCATATCC	1759749-1759768 (CP054134)

bioRxiv preprint doi: https://doi.org/10.1101/2020.07.17.206995; this version posted November 14, 2020. The copyright holder for this preprint (which was not certified by peer review) is the author/funder. All rights reserved. No reuse allowed without permission.

IE12_1078	D.3	GCTCCAAAGACTGAAACAAC	1078994-1079013 (CP054134)
	D.4	TAATTATCTTTCGTTACCTT	1079738-1079757 (CP054134)
IE12_1004	D.5	TGAGGAGAAGAAGACAACAG	1007350-1007369 (CP054134)
	D.6	CGATATTTGAAATGACCAT	1007831-1007849 (CP054134)
IE18_1262	D.7	CGTCAGAAAAATCTAAGGAAG	1239935-1239955 (JABTEW010000000)
	D.8	CTTGATAATCACCTTCTTCTG	1239569-1239589 (JABTEW010000000)
IE18_1284	D.9	GTCCTGATCTTCTTCGCGATG	1257593-1257613 (JABTEW010000000)
	D.10	ATTCAAAGTAGAACCATATCC	1257030-1257050 (JABTEW010000000)
IE18_2031	D.11	CGCCTTCAGGAGAGAACACG	2019219-2019238 (JABTEW010000000)
	D.12	GCATCATCAAATGCTTGCTT	2018570-2018589 (JABTEW010000000)
aad9	Sp.1	CGATTTTCGTTCGTGAATAC	5399-5418 (KM009065)
	Sp.2	TATGCAAGGGTTTATTGTTTTC	4265-4286 (KM009065)
Janus	J.1	GGGCCCCTTTCCTTATGCTT	773-796 (AF411920.1)
	J.2	CCGTTTGATTTTTAATGGATAATG	2086-2105 (AF411920.1)
Cat	Ca.1	TAGTTCAACAAAGGAAAATTGGATAA	4727-4822 (MN956986.1)
	Ca.2	ACGGGGCAGGTTAGTGACAT	3951-3970 (MN956986.1)
rpoB	R.1	AARYTIGGMCCTGAAGAAAT[h]	655075-655095 (CP054134)
	R.2	TGIARTTTRTCATCAACCATGTG[h]	655793-655806 (CP054134)

[a]Underlining indicates nucleotides introduced to allow In-Fusion cloning into the pJET2.1/Blunt.
[b]Underlining indicates nucleotides introduced to allow In-Fusion cloning with *cat* (chloramphenicol resistance cassette).
[c]Underlining indicates nucleotides introduced to allow In-Fusion cloning with *aad9* (spectinomycin resistance cassette).
[d]Underlining indicates nucleotides introduced to allow In-Fusion cloning into the pGEX-5X-3 vector.
[e]Underlining indicates nucleotides introduced to allow In-Fusion cloning into the pOPINF vector.
[f]Underlining indicates nucleotides introduced to allow In-Fusion cloning into the pDrive vector.
[g]Underlining indicates nucleotides introduced to allow In-Fusion cloning into the pABG5 vector.
[h]R, purine (adenine or guanine); Y, pyrimidine (thymine or cytosine); I, inosine; M, adenine or cytosine.

The presence of the genes encoding potential carbohydrate binding adhesins in the five different IE-isolates was determined by PCR using the corresponding primer pairs (Table 2).

RNA isolation and RT-PCR

RNA isolation was conducted with the RNeasy mini kit (Qiagen) as previously reported [39]. Briefly, the cell pellet of 1 mL of bacterial culture grown to an OD_{600} of 0.4 was washed twice with phosphate-buffered saline (PBS) and resuspended in 540 µL of acid phenol containing 6 µL of 10% SDS. After flash-freezing, the samples were thawed at 70°C and then 540 µL of chloroform and 100 µL of Tris-EDTA buffer were added.

bioRxiv preprint doi: https://doi.org/10.1101/2020.07.17.206995; this version posted November 14, 2020. The copyright holder for this preprint (which was not certified by peer review) is the author/funder. All rights reserved. No reuse allowed without permission.

688 Samples were further incubated for 30 minutes at 70°C and vortexed every 5 minutes.
689 RLT buffer was added to the sample, vortexed and centrifuged at 12,000 x g for 12
690 minutes. The aqueous phase was mixed with 70% ethanol, loaded into a RNeasy
691 minicolumn (Qiagen) and further processed following the manufacturer's instructions.
692 RNA was treated with DNase I (Invitrogen) and further purified with the RNeasy mini kit.
693 cDNA was synthesized from 1 µg of RNA using SuperScript II reverse transcriptase
694 (Invitrogen) according to the manufacturer's instructions.
695
696 Expression of *srtA, asaA* and *csh-like* was confirmed with the primer pairs S.1 - S.2, A.1
697 - A.2 and C.1 - C.2, respectively. To exclude possible polar effects caused by the
698 deletion of *srtA, asaA* or *csh-like*, expression of the genes encoded downstream was
699 confirmed using primer pairs S.7 - S.8, A.5 - A.6 and C.7 - C.8, respectively. In all
700 cases, *rpoB* was used as a positive control (primers R.1 and R.2).
701
702 **Plasmid construction**
703 The plasmid constructs used to generate the *S. oralis* subsp. *oralis* Δ*srtA,* Δ*asaA* and
704 Δ*csh-like* mutants are described below. The regions upstream and downstream of the
705 *srtA* gene were amplified from *S. oralis* subsp. *oralis* gDNA using the primer pairs S.3 -
706 S.4, and S.5 - S.6, respectively. The spectinomycin cassette was amplified with primers
707 Sp.1 and Sp.2. These three fragments were cloned into EcoRI-digested pDrive (Qiagen)
708 using the In-Fusion HD EcoDry cloning kit (Takara Bio), resulting in the plasmid
709 pDriveΔ*srtA*. The construct to generate the *asaA* mutant was generated by amplifying a
710 1.5 kb fragment, corresponding to the NRR of *asaA,* with primers A.3 and A.4. The

bioRxiv preprint doi: https://doi.org/10.1101/2020.07.17.206995; this version posted November 14, 2020. The copyright holder for this preprint (which was not certified by peer review) is the author/funder. All rights reserved. No reuse allowed without permission.

711 product was blunt-end ligated into the pJET1.2/Blunt PCR cloning vector (Thermo
712 Fisher Scientific). The resulting plasmid was digested with HincII, which removed ~400
713 bp of *asaA*, then the Janus cassette was blunt-end ligated into this construct, generating
714 the pJETΔ*asaA* plasmid. A 1.9 kb region, corresponding to the NRR-encoding region of
715 *csh-like,* was amplified using primers C.3 and C.4, and blunt-end ligated into pJET1.2.
716 The generated construct was used as a template for inverse PCR with primers C.5 and
717 C.6. The resulting PCR product was blunt-end ligated to the spectinomycin resistance
718 cassette, generating the pJETΔ*csh* plasmid. For complementation studies, the *srtA*
719 gene was amplified by PCR using primers S.10 and S.11 and cloned by In-fusion in
720 pABG5.
721
722 The plasmids used to generate the deletion mutants lacking the NRR or Siglec and
723 Unique domains are described below. First, to generate a strain lacking the NRR (see
724 below), we constructed the plasmid pJET*asaA*_NRR::Cm. To this end, two PCR
725 products comprising ~800 bp upstream of the promoter of *asaA* (Up) and ~400 bp
726 downstream of codon 704 (Dn) were amplified using primer pairs A.7 - A.8 and A.9 -
727 A.10, respectively. The chloramphenicol cassette (Cm) was amplified using primers
728 Ca.1 and Ca.2. These three PCR fragments (Up-Cm-Dn) were cloned into
729 pJET1.2/Blunt using the In-Fusion HD EcoDry cloning kit. Next, we constructed a
730 plasmid in which a spectinomycin resistance cassette was introduced before the
731 promoter of *asaA*. We did so by cloning the following PCR products into pJET1.2/Blunt:
732 a fragment comprising ~800 bp upstream the *asaA* promoter, amplified using primers
733 A.7 and A.11, the spectinomycin resistant cassette and a 2.7 kb DNA region (amplified

bioRxiv preprint doi: https://doi.org/10.1101/2020.07.17.206995; this version posted November 14, 2020. The copyright holder for this preprint (which was not certified by peer review) is the author/funder. All rights reserved. No reuse allowed without permission.

734 using primers A.12 and A.10) comprising the promoter and the first 846 codons of *asaA*.
735 The resulting construct was used as a template to amplify two PCR fragments using
736 primer pairs A.7 - A.13 and A.14 - A.10 (primer A.13 and A.14 introduce a 3xFLAG tag)
737 that were cloned by In-Fusion into pJET1.2/Blunt. The resulting plasmid was named
738 pJET*asaA*WT-3F. Finally, to generate the pJET*asaA*ΔNRR-3F and pJET*asaA*ΔSU-3F
739 constructs, two PCR fragments for each construct were amplified using gDNA from IE12
740 *asaA* WT-3F as a template with the following primer pairs: A.7 - A.15/A.16 - A.10 and
741 A.7 - A.17/A.19 - A.10, respectively. These PCR fragments were cloned by In-Fusion
742 into pJET1.2/Blunt.
743
744 For co-infection studies in a rabbit model of IE we generated an isogenic IE12 strain
745 resistant to chloramphenicol (IE12 Cm^r). To that end, we used primers I.1 and I.2 to
746 amplify a conserved intergenic region (IR) between two convergent genes encoding: a
747 TrkH family potassium uptake protein (TrkG) and an oligopeptide ABC transporter ATP-
748 binding protein (OppF). The product was blunt-end ligated into pJET1.2 and used as a
749 template for inverse PCR with primers I.3 and I.4. The resulting PCR product was blunt-
750 end ligated to the chloramphenicol resistance cassette (pJETIR::Cm).
751
752 For protein purification, pGEX_So_AsaA_NRR, pGEX_So_AsaA_SU_1-2 and
753 pGEX_Gh_AsaA_NRR were constructed as follows. The full-length NRRs of AsaA from
754 *S. oralis* subsp. *oralis* IE12 and *G. haemolysans* M341 (comprising amino acids 37 to
755 702 and 50 to 739, respectively), were amplified from gDNA using primers A.19 - A.20
756 and A.21 - A.22, respectively. A region comprising both Siglec-like and Unique domains

bioRxiv preprint doi: https://doi.org/10.1101/2020.07.17.206995; this version posted November 14, 2020. The copyright holder for this preprint (which was not certified by peer review) is the author/funder. All rights reserved. No reuse allowed without permission.

of So_AsaA (amino acids 179-714) was amplified using primers A.23 - A.24. The resulting PCR products were cloned by In Fusion into pGEX-5X-3, which allows the expression of N-terminally GST-tagged proteins. The construct pOPINF_18_Csh_NRR was design to express the NRR of the Csh-like protein with an N-terminal His-tag. Briefly, a PCR fragment, comprising codons 42 to 666, was amplified using primers C.9 and C.10 and cloned into pOPINF using the In-Fusion HD EcoDry cloning kit (Takara Bio).

All constructs were confirmed by PCR and sequencing to verify that no spurious mutations had been introduced.

Generation of mutants in *S. oralis* subsp. *oralis*

IE12 Δ*srtA*, IE12 Δ*asaA* and IE12 Cm^r were generated by transforming the plasmids pDriveΔ*srtA*, pJETΔ*asaA* and pJETIR::Cm into IE12. While for the IE18 *srtA* and IE18 *csh-like* mutants, pDriveΔ*srtA* and pJETΔ*csh* plasmids were transformed into IE18. Briefly, *S. oralis* subsp. *oralis* strains were grown in C+Y media to an OD_{600} of 0.1 and then diluted in fresh media (1:20). Competence was induced by the addition of a competence stimulating peptide (2 µg/mL) and 1 mM $CaCl_2$ [9]. Approximately 100 ng of plasmid was added and the transformations were then incubated for 2 h at 37°C. Transformants were selected on TSA plates with the appropriate antibiotics. All desired mutations were confirmed by PCR using flanking primers (A.25, C.11, S.9 and I.5) in combination with primers for the antibiotic resistance cassette included in each mutant (J.1, Sp.2, Sp1 and Ca.2).

bioRxiv preprint doi: https://doi.org/10.1101/2020.07.17.206995; this version posted November 14, 2020. The copyright holder for this preprint (which was not certified by peer review) is the author/funder. All rights reserved. No reuse allowed without permission.

To complement the *srtA* mutants, the plasmid pABG5-*srtA* was transformed by electroporation as previously described [91]. Briefly, cells were grown in THY supplemented with 20 mM glycine to an OD_{600} of 0.2, harvested by centrifugation and resuspended in ice-cold electroporation medium (272 mM glucose, 1 mM $MgCl_2$, pH 6.5). DNA was added to an aliquot of cells and transformed by electroporation. After 2 h incubation in THY at 37°C cells were plated into TSA plates with the appropriate antibiotics.

To generate the deletion mutants lacking the NRR or Siglec-like and Unique domains of AsaA we first generated an intermediate strain in which the NRR of AsaA was replaced with the chloramphenicol cassette. To this end, the pJET*asaA*_NRR::Cm construct was transformed into *S. oralis* subsp. *oralis* IE12 as described above. The resulting strain (IE12 *asaA*_NRR::Cm) was then transformed with the pJET*asaA*WT-3F, pJET*asaA*ΔNRR-3F or pJET*asaA*ΔSU-3F plasmids. The resulting colonies were selected for the resistance to spectinomycin and sensitivity to chloramphenicol. Desired mutations were confirmed by sequencing.

The genetic background of all mutants was confirmed by repetitive extragenic palindromic PCR [92]. Any possible growth defects were excluded by conducting growth assays on rich medium as previously described [39].

Protein overproduction and purification

bioRxiv preprint doi: https://doi.org/10.1101/2020.07.17.206995; this version posted November 14, 2020. The copyright holder for this preprint (which was not certified by peer review) is the author/funder. All rights reserved. No reuse allowed without permission.

803 The N-terminally His-tagged CBM40 and the two tandem CBM71 domains (CBM71-1.2)
804 from *Streptococcus pneumoniae* neuraminidase NanA and β-galactosidase BgaA,
805 respectively, were purified by nickel affinity chromatography as described previously
806 [29, 39].
807
808 To purify GST or the GST-tagged NRRs of So_AsaA and Gh_AsaA, plasmids pGEX-
809 5X-3, pGEX_So_AsaA_NRR pGEX_So_AsaA_SU1-2 or pGEX_Gh_AsaA_NRR were
810 transformed into the *E. coli* host strain BL21 (DE3) (Invitrogen). Overnight cultures of
811 the transformed strains, grown at 37°C with constant shaking, were used to inoculate
812 fresh LB containing the appropriate antibiotics. Growth was continued under the same
813 conditions until an OD_{600} of 0.8 was reached. At this point, protein production was
814 induced by the addition of isopropyl β-D-1-thiogalactopyranoside (IPTG) to a final
815 concentration of 0.5 mM followed by a 4 h incubation at 30°C with constant shaking.
816 Cells were harvested by centrifugation and lysed using a French Press. Cleared cell
817 lysates were used for further purification by affinity chromatography. The cleared cell
818 lysates were incubated overnight with glutathione-Sepharose 4B beads (GE Healthcare
819 Life Sciences) in the presence of 5 mM dithiothreitol (DTT) at 4°C with gentle agitation.
820 The beads were extensively washed with 50 mM Tris-HCl, 150 mM NaCl, pH 8.0.
821 Finally, GST and GST-tagged proteins were eluted with 10 mM reduced glutathione.
822
823 The purification of the NRR of Csh-like was carried out as previously described for the
824 NR2 of CshA [36]. Briefly, protein expression was induced by the addition of 1 mM IPTG
825 for 16 h at 18°C. The His-tagged protein was purified from the cleared cell lysate by

bioRxiv preprint doi: https://doi.org/10.1101/2020.07.17.206995; this version posted November 14, 2020. The copyright holder for this preprint (which was not certified by peer review) is the author/funder. All rights reserved. No reuse allowed without permission.

826 nickel affinity chromatography (Ni-NTA agarose beads, Invitrogen). After washing with
827 increasing concentrations of imidazole, proteins were eluted with 200 mM imidazole in
828 20 mM Tris-HCl, 150 mM NaCl, pH 8.
829
830 Purified proteins were dialyzed overnight against PBS containing 1 mM DTT. Size and
831 purity were verified by Coomassie blue-stained SDS-PAGE. Protein concentration was
832 determined using the absorbance at 280 nm and the extinction coefficient.
833
834 Proper folding of the Csh_NRR was confirmed by CD-spectroscopy. CD-spectra of
835 Csh_NRR in PBS was collected using a Jasco J-815 spectrometer, using a 1 mm path
836 length cuvette, with a wavelength interval of 0.5 nm. Data was analyzed and plotted
837 using CAPITO (CD Analysis and Plotting Tool) [93].
838
839 **Platelet isolation**
840 Platelet isolation has been described previously and was performed with slight
841 modifications [9]. Blood from healthy donors was collected in acid citrate dextrose
842 solution (75 mM sodium citrate, 39 mM citric acid, 135 mM dextrose, pH 7.4). Pooled
843 platelet rich plasma was collected after centrifugation of blood samples at 200 x g for 20
844 minutes and mixed 1:1 with HEP buffer (140 mM NaCl, 2.7 mM KCl, 3.8 mM HEPES, 5
845 mM EDTA, pH 7.4). Platelets were collected by centrifugation at 800 x g for 20 minutes
846 with no brake applied and washed twice with platelet wash buffer (10 mM sodium
847 citrate, 150 mM NaCl, 1 mM EDTA, 1% (w/v) dextrose, pH 7.4). Platelets were fixed
848 with 1% paraformaldehyde for 10 minutes at room temperature and then washed three

bioRxiv preprint doi: https://doi.org/10.1101/2020.07.17.206995; this version posted November 14, 2020. The copyright holder for this preprint (which was not certified by peer review) is the author/funder. All rights reserved. No reuse allowed without permission.

849 times with PBS. Platelets were resuspended in PBS at $1x10^7$ cells per mL. Flat-
850 bottomed 96-well microtiter plates were coated with 100 µL of platelets for 1 h at 37°C.
851 Control wells were coated with 1% (w/v) bovine serum albumin (BSA) in PBS. Unbound
852 platelets were removed by two PBS washes. Platelets-coated plates were stored at 4°C
853 until further use.
854
855 **Adherence assays**
856 Where indicated, platelet-coated wells were pretreated with 0.005 U of *Clostridium*
857 *perfringens* neuraminidase (Sigma) for 30 minutes at 37°C, control wells were incubated
858 with PBS. After washing with PBS, all wells were blocked with 3% BSA in PBS for 1 h at
859 37°C.
860
861 Bacteria were grown in THY to an OD_{600} of 0.5 $\pm$ 0.05. Approximately $2x10^5$ bacteria in
862 PBS were allowed to bind to fixed platelets at 37°C for 60 minutes. Three washes with
863 PBS were performed to remove non-adherent bacteria and then adherent bacteria were
864 lifted with 0.25% trypsin-1 mM EDTA at 37°C for 15 minutes. CFU counts were
865 performed by serial dilution.
866
867 To test the effect of CBM40, CBM71-1.2, Csh_NRR, AsaA_NRR, AsaA_SU1-2 and
868 Gh_AsaA_NRR on bacterial binding to platelets, soluble protein was added to the
869 bacterial inoculum at the concentrations indicated in each experiment.
870
871 **Platelet binding to immobilized protein.**

bioRxiv preprint doi: https://doi.org/10.1101/2020.07.17.206995; this version posted November 14, 2020. The copyright holder for this preprint (which was not certified by peer review) is the author/funder. All rights reserved. No reuse allowed without permission.

872 Binding assays were performed in 96-well plates (Nunc MaxiSorp) coated overnight at
873 4°C with 100 µL of 5 µM AsaA_NRR, AsaA_SU_1-2 or GST. After washing to remove
874 unbound protein with PBS, wells were blocked with 1% BSA at 37°C for 1 h. Two
875 washes with PBS were performed before adding 100 µL of platelets ($1x10^7$ platelets per
876 mL) pretreated with PBS or neuraminidase. After 2 h of incubation at 37°C wells were
877 washed three times with PBS and then fixed with 90% ethanol. Fixed platelets were
878 stained with 0.1% crystal violet and imaged using a Nikon eclipse Ti inverted
879 microscope with a 40x objective. The number of platelets in each field was quantified
880 using ImageJ [94].
881
882 **Detection of AsaA-3xFLAG.**
883 The production of the AsaA deletion mutants was verified by western blot. All strains
884 were grown to an OD_{600} of 0.5. After harvesting cells by centrifugation, the pellet was
885 resuspended in PBS containing 1% sodium deoxycholate and 1% SDS and normalized
886 according to the OD (PBS volume = OD_{600} x 400). Ten microliters of the whole cell
887 lysates were spotted onto nitrocellulose membrane. After an hour, the membrane was
888 blocked for 1 h with 1% BSA in PBS. Three washes with tTBS (50 mM Tris, 150 mM
889 NaCl and 0.1% Tween 20) were performed before incubating the membrane with the
890 anti-FLAG antibody 1:5000 for 1 h (Sigma). Next, after three washes with tTBS, the
891 membrane was incubated with the secondary antibody 1:5000 for 1 h (HRP-coupled
892 anti-rabbit IgG, Invitrogen). Protein detection was performed with the SuperSignal West
893 Pico Plus kit according to the manufacturer's instructions (Thermo Scientific).
894

bioRxiv preprint doi: https://doi.org/10.1101/2020.07.17.206995; this version posted November 14, 2020. The copyright holder for this preprint (which was not certified by peer review) is the author/funder. All rights reserved. No reuse allowed without permission.

Detection of the AsaA-3xFLAG deletion versions on the surface of IE12 was done with immunofluorescence. Cells were grown in THY until an OD_{600} of 0.5 was reached, then Nile red was added to the media (final concentration 1 ug/mL). After an additional 20 minute incubation, the cells were harvested by centrifugation. The cell pellets were washed three times with PBS and then fixed for 20 minutes with 40% methanol. Cells were washed with PBS and then incubated with anti-FLAG antibody 1:200 (Sigma) for 1 h at room temperature. After three washes with PBS cells were incubated with the secondary antibody 1:200 (Alexa Fluor 488, goat anti-rabbit IgG, Invitrogen) for 1 h. Finally, cells were washed three times and imaged on a LSM 800 confocal microscope (Zeiss, Germany). Images were rendered with Zeiss Zen software (Zeiss, Germany).

Rabbit model of IE

The rabbit model employed for virulence assays has been described previously [41] and was performed with minor variations. Briefly, specific-pathogen-free, male New Zealand White rabbits weighing 2 - 3 kg and supplied by Charles Rivers Laboratories (experiment 1) or RSI Biotechnology (experiment 2) were used. Animals were anesthetized prior to surgery, which involved insertion of a catheter through the right carotid artery to the aortic valve or left ventricle to induce minor damage to the endothelium. Bacterial strains were cultured separately, then washed and combined in 0.5 mL PBS for co-inoculation of approximately $1x10^7$ CFU of each strain into a peripheral ear vein two days after surgery. Remaining cells were sonicated to disrupt clumps and chains and plated on BHI plates with selective antibiotics using an Eddy Jet 2 spiral plater (Neutec Group, Inc.). The following day, the animals were euthanized and

bioRxiv preprint doi: https://doi.org/10.1101/2020.07.17.206995; this version posted November 14, 2020. The copyright holder for this preprint (which was not certified by peer review) is the author/funder. All rights reserved. No reuse allowed without permission.

vegetations in or near the aortic valves were removed, homogenized in PBS, sonicated, and plated, as for the inoculum. Plates were incubated at 37°C in Anoxomat jars for two days prior to counting colonies. Results were normalized to account for small (≤ 10%) differences in the inoculum sizes of the competing strains.

Bacterial binding to immobilized fibrinogen and fibronectin.

Assays were performed in 96-well plates (Nunc MaxiSorp) coated overnight at 4°C with 100 µL of fibrinogen (20 µM, Invitrogen) or fibronectin (50 µM, EMD Millipore Calbiochem); control wells were coated with 3% BSA. After washing to remove unbound protein, wells were blocked for 1 h at 37°C with 3% BSA. Approximately $2x10^5$ bacteria in PBS were allowed to bind at 37°C for 2 h. Wells were washed three times with PBS and then adherent bacteria were lifted with 0.25% trypsin-1 mM EDTA at 37°C for 15 minutes. CFU counts were performed by serial dilutions.

***In silico* analysis**

Protein homology and structure were predicted using the HHPred server [37]. The AsaA three-dimensional model was built using the SWISS-MODEL server [95]. Protein structures were edited for visualization using PyMOL (The PyMOL Molecular Graphics System, Version 2.0 Schrödinger, LLC). Multiple sequence alignments were carried out using Clustal Omega [96].

Statistical analysis

bioRxiv preprint doi: https://doi.org/10.1101/2020.07.17.206995; this version posted November 14, 2020. The copyright holder for this preprint (which was not certified by peer review) is the author/funder. All rights reserved. No reuse allowed without permission.

In vitro data are presented as mean of at least three independent experiments ± standard deviation (SD). Data analysis was performed using GraphPad Prism. Two-tailed Student's t-test were used to determine differences in bacterial and platelet adhesion. For rabbit studies, log-transformed values were analyzed by paired Student's t-test.

Accession number(s)

The MLSA sequences for the five *S. oralis* subsp. *oralis* isolates were submitted to GenBank and have the accession numbers MT551124 to MT551158. Genome assemblies of *S. oralis* subsp. oralis strains ATCC10557, IE12 and IE18 were deposited at GenBank under the accession numbers CP054135, CP054134 and JABTEW010000000, respectively. The data have been deposited with links to BioProject accession number PRJNA635656 at the NCBI BioProject database (https://www.ncbi.nlm.nih.gov/bioproject/).

Ethics Statement

Blood draws involved the informed written consent of donors, with ethical approval obtained from the Institutional Review Board of Nationwide Children's Hospital under protocol number IRB16-01173. For the endocarditis model, rabbits were premedicated with acepromazine, buprenorphine, and bupivacaine at the incision site, and then anesthetized for surgery with isoflurane and sevoflurane. Buprenorphine SR LAB (ZooPharm) was provided for post-surgical analgesia. Euthanasia was achieved by administration of Euthasol (pentobarbital sodium and phenytoin sodium solution; Virbac

bioRxiv preprint doi: https://doi.org/10.1101/2020.07.17.206995; this version posted November 14, 2020. The copyright holder for this preprint (which was not certified by peer review) is the author/funder. All rights reserved. No reuse allowed without permission.

AH Inc.). All procedures performed in relation to the rabbit endocarditis model were approved by the Institutional Animal Care and Use Committee of Virginia Commonwealth University under protocol number AM10030, and were consistent with United States Department of Agriculture Animal Welfare Act and Regulations, the United States Office of Laboratory Animal Welfare Policies and Laws, and The Guide for the Care and Use of Laboratory Animals published by the National Research Council.

Acknowledgments

We thank Shannon Green, Karina Kunka, Tanya Puccio, and Nicai Zollar for technical assistance with the rabbit studies. We are thankful to M. Kilian for providing an MLSA database to confirm species assignment. We thank Alicia Friedman of the Biophysical Interaction and Characterization Facility at The Ohio State University for her help with circular dichroism and Frank Robledo-Avila for his technical help with microscopy analysis. *Gemella haemolysans* M341 was obtained through BEI Resources, NIAID, NIH, as part of the Human Microbiome Project.

References

1. Heller D, Helmerhorst EJ, Gower AC, Siqueira WL, Paster BJ, Oppenheim FG. Microbial Diversity in the Early In Vivo-Formed Dental Biofilm. Appl Environ Microbiol. 2016;82(6):1881-8.
2. Sulyanto RM, Thompson ZA, Beall CJ, Leys EJ, Griffen AL. The Predominant Oral Microbiota Is Acquired Early in an Organized Pattern. Sci Rep. 2019;9(1):10550.
3. Cahill TJ, Prendergast BD. Infective endocarditis. Lancet. 2016;387(10021):882-93.
4. Knox KW, Hunter N. The role of oral bacteria in the pathogenesis of infective endocarditis. Aust Dent J. 1991;36(4):286-92.
5. Lockhart PB, Brennan MT, Sasser HC, Fox PC, Paster BJ, Bahrani-Mougeot FK. Bacteremia associated with toothbrushing and dental extraction. Circulation. 2008;117(24):3118-25.

bioRxiv preprint doi: https://doi.org/10.1101/2020.07.17.206995; this version posted November 14, 2020. The copyright holder for this preprint (which was not certified by peer review) is the author/funder. All rights reserved. No reuse allowed without permission.

6. Holland TL, Baddour LM, Bayer AS, Hoen B, Miro JM, Fowler VG, Jr. Infective endocarditis. Nat Rev Dis Primers. 2016;2:16059.
7. Naveen Kumar V, van der Linden M, Menon T, Nitsche-Schmitz DP. Viridans and bovis group streptococci that cause infective endocarditis in two regions with contrasting epidemiology. Int J Med Microbiol. 2014;304(3-4):262-8.
8. Werdan K, Dietz S, Loffler B, Niemann S, Bushnaq H, Silber RE, et al. Mechanisms of infective endocarditis: pathogen-host interaction and risk states. Nat Rev Cardiol. 2014;11(1):35-50.
9. Singh AK, Woodiga SA, Grau MA, King SJ. Streptococcus oralis Neuraminidase Modulates Adherence to Multiple Carbohydrates on Platelets. Infect Immun. 2017;85(3).
10. Bensing BA, Loukachevitch LV, McCulloch KM, Yu H, Vann KR, Wawrzak Z, et al. Structural Basis for Sialoglycan Binding by the Streptococcus sanguinis SrpA Adhesin. J Biol Chem. 2016;291(14):7230-40.
11. Loukachevitch LV, Bensing BA, Yu H, Zeng J, Chen X, Sullam PM, et al. Structures of the Streptococcus sanguinis SrpA Binding Region with Human Sialoglycans Suggest Features of the Physiological Ligand. Biochemistry. 2016;55(42):5927-37.
12. Bensing BA, Lopez JA, Sullam PM. The Streptococcus gordonii surface proteins GspB and Hsa mediate binding to sialylated carbohydrate epitopes on the platelet membrane glycoprotein Ibalpha. Infect Immun. 2004;72(11):6528-37.
13. Takamatsu D, Bensing BA, Cheng H, Jarvis GA, Siboo IR, Lopez JA, et al. Binding of the Streptococcus gordonii surface glycoproteins GspB and Hsa to specific carbohydrate structures on platelet membrane glycoprotein Ibalpha. Mol Microbiol. 2005;58(2):380-92.
14. Siboo IR, Chambers HF, Sullam PM. Role of SraP, a Serine-Rich Surface Protein of Staphylococcus aureus, in binding to human platelets. Infect Immun. 2005;73(4):2273-80.
15. Pyburn TM, Bensing BA, Xiong YQ, Melancon BJ, Tomasiak TM, Ward NJ, et al. A structural model for binding of the serine-rich repeat adhesin GspB to host carbohydrate receptors. PLoS Pathog. 2011;7(7):e1002112.
16. Lizcano A, Sanchez CJ, Orihuela CJ. A role for glycosylated serine-rich repeat proteins in gram-positive bacterial pathogenesis. Mol Oral Microbiol. 2012;27(4):257-69.
17. Zhou M, Wu H. Glycosylation and biogenesis of a family of serine-rich bacterial adhesins. Microbiology. 2009;155(Pt 2):317-27.
18. Ramboarina S, Garnett JA, Zhou M, Li Y, Peng Z, Taylor JD, et al. Structural insights into serine-rich fimbriae from Gram-positive bacteria. J Biol Chem. 2010;285(42):32446-57.
19. Deng L, Bensing BA, Thamadilok S, Yu H, Lau K, Chen X, et al. Oral streptococci utilize a Siglec-like domain of serine-rich repeat adhesins to preferentially target platelet sialoglycans in human blood. PLoS Pathog. 2014;10(12):e1004540.
20. Bensing BA, Loukachevitch LV, Agarwal R, Yamakawa I, Luong K, Hadadianpour A, et al. Selectivity and engineering of the sialoglycan-binding spectrum in Siglec-like adhesins. bioRxiv. 2019:796912.
21. Bensing BA, Khedri Z, Deng L, Yu H, Prakobphol A, Fisher SJ, et al. Novel aspects of sialoglycan recognition by the Siglec-like domains of streptococcal SRR glycoproteins. Glycobiology. 2016;26(11):1222-34.
22. Urano-Tashiro Y, Takahashi Y, Oguchi R, Konishi K. Two Arginine Residues of Streptococcus gordonii Sialic Acid-Binding Adhesin Hsa Are Essential for Interaction to Host Cell Receptors. PLoS One. 2016;11(4):e0154098.
23. Xiong YQ, Bensing BA, Bayer AS, Chambers HF, Sullam PM. Role of the serine-rich surface glycoprotein GspB of Streptococcus gordonii in the pathogenesis of infective endocarditis. Microb Pathog. 2008;45(4):297-301.

bioRxiv preprint doi: https://doi.org/10.1101/2020.07.17.206995; this version posted November 14, 2020. The copyright holder for this preprint (which was not certified by peer review) is the author/funder. All rights reserved. No reuse allowed without permission.

1036 24. Bensing BA, Li L, Yakovenko O, Wong M, Barnard KN, Iverson TM, et al. Recognition of specific
1037 sialoglycan structures by oral streptococci impacts the severity of endocardial infection. PLoS Pathog.
1038 2019;15(6):e1007896.
1039 25. Takahashi Y, Takashima E, Shimazu K, Yagishita H, Aoba T, Konishi K. Contribution of sialic acid-
1040 binding adhesin to pathogenesis of experimental endocarditis caused by Streptococcus gordonii DL1.
1041 Infect Immun. 2006;74(1):740-3.
1042 26. Wong A, Grau MA, Singh AK, Woodiga SA, King SJ. Role of Neuraminidase-Producing Bacteria in
1043 Exposing Cryptic Carbohydrate Receptors for Streptococcus gordonii Adherence. Infect Immun.
1044 2018;86(7).
1045 27. Yang L, Connaris H, Potter JA, Taylor GL. Structural characterization of the carbohydrate-binding
1046 module of NanA sialidase, a pneumococcal virulence factor. BMC Struct Biol. 2015;15:15.
1047 28. Bensing BA, Seepersaud R, Yen YT, Sullam PM. Selective transport by SecA2: an expanding family
1048 of customized motor proteins. Biochim Biophys Acta. 2014;1843(8):1674-86.
1049 29. Singh AK, Pluvinage B, Higgins MA, Dalia AB, Woodiga SA, Flynn M, et al. Unravelling the
1050 multiple functions of the architecturally intricate Streptococcus pneumoniae beta-galactosidase, BgaA.
1051 PLoS Pathog. 2014;10(9):e1004364.
1052 30. Marraffini LA, Dedent AC, Schneewind O. Sortases and the art of anchoring proteins to the
1053 envelopes of gram-positive bacteria. Microbiol Mol Biol Rev. 2006;70(1):192-221.
1054 31. Schneewind O, Missiakas D. Sec-secretion and sortase-mediated anchoring of proteins in Gram-
1055 positive bacteria. Biochim Biophys Acta. 2014;1843(8):1687-97.
1056 32. Navarre WW, Schneewind O. Proteolytic cleavage and cell wall anchoring at the LPXTG motif of
1057 surface proteins in gram-positive bacteria. Mol Microbiol. 1994;14(1):115-21.
1058 33. McNab R, Holmes AR, Clarke JM, Tannock GW, Jenkinson HF. Cell surface polypeptide CshA
1059 mediates binding of Streptococcus gordonii to other oral bacteria and to immobilized fibronectin. Infect
1060 Immun. 1996;64(10):4204-10.
1061 34. Holmes AR, McNab R, Jenkinson HF. Candida albicans binding to the oral bacterium
1062 Streptococcus gordonii involves multiple adhesin-receptor interactions. Infect Immun.
1063 1996;64(11):4680-5.
1064 35. McNab R, Jenkinson HF, Loach DM, Tannock GW. Cell-surface-associated polypeptides CshA and
1065 CshB of high molecular mass are colonization determinants in the oral bacterium Streptococcus
1066 gordonii. Mol Microbiol. 1994;14(4):743-54.
1067 36. Back CR, Sztukowska MN, Till M, Lamont RJ, Jenkinson HF, Nobbs AH, et al. The Streptococcus
1068 gordonii Adhesin CshA Protein Binds Host Fibronectin via a Catch-Clamp Mechanism. J Biol Chem.
1069 2017;292(5):1538-49.
1070 37. Soding J, Biegert A, Lupas AN. The HHpred interactive server for protein homology detection and
1071 structure prediction. Nucleic Acids Res. 2005;33(Web Server issue):W244-8.
1072 38. Christner M, Franke GC, Schommer NN, Wendt U, Wegert K, Pehle P, et al. The giant
1073 extracellular matrix-binding protein of Staphylococcus epidermidis mediates biofilm accumulation and
1074 attachment to fibronectin. Mol Microbiol. 2010;75(1):187-207.
1075 39. Ronis A, Brockman K, Singh AK, Gaytan M, Wong A, McGrath S, et al. Streptococcus oralis subsp.
1076 dentisani produces mono-lateral serine rich repeat protein fibrils one of which contributes to saliva
1077 binding via sialic acid. Infect Immun. 2019.
1078 40. Linke C, Siemens N, Oehmcke S, Radjainia M, Law RH, Whisstock JC, et al. The extracellular
1079 protein factor Epf from Streptococcus pyogenes is a cell surface adhesin that binds to cells through an N-
1080 terminal domain containing a carbohydrate-binding module. J Biol Chem. 2012;287(45):38178-89.
1081 41. Crump KE, Bainbridge B, Brusko S, Turner LS, Ge X, Stone V, et al. The relationship of the
1082 lipoprotein SsaB, manganese and superoxide dismutase in Streptococcus sanguinis virulence for
1083 endocarditis. Mol Microbiol. 2014;92(6):1243-59.

bioRxiv preprint doi: https://doi.org/10.1101/2020.07.17.206995; this version posted November 14, 2020. The copyright holder for this preprint (which was not certified by peer review) is the author/funder. All rights reserved. No reuse allowed without permission.

1084 42. Lowrance JH, Baddour LM, Simpson WA. The role of fibronectin binding in the rat model of
1085 experimental endocarditis caused by Streptococcus sanguis. J Clin Invest. 1990;86(1):7-13.
1086 43. Que YA, Haefliger JA, Piroth L, Francois P, Widmer E, Entenza JM, et al. Fibrinogen and
1087 fibronectin binding cooperate for valve infection and invasion in Staphylococcus aureus experimental
1088 endocarditis. J Exp Med. 2005;201(10):1627-35.
1089 44. Fitzgerald JR, Foster TJ, Cox D. The interaction of bacterial pathogens with platelets. Nat Rev
1090 Microbiol. 2006;4(6):445-57.
1091 45. Khan R, Urban C, Rubin D, Segal-Maurer S. Subacute endocarditis caused by Gemella
1092 haemolysans and a review of the literature. Scand J Infect Dis. 2004;36(11-12):885-8.
1093 46. Sadaune L, Roca F, Bordage M, Le Guillou V, Lesourd A, Michel A. Benefits of a Pre-Treatment
1094 Comprehensive Geriatric Assessment in a Rare Case of Gemella Haemolysans Endocarditis in an 86-Year-
1095 Old Patient and a Review of the Literature. Medicina (Kaunas). 2019;55(6).
1096 47. Youssef D, Youssef I, Marroush TS, Sharma M. Gemella endocarditis: A case report and a review
1097 of the literature. Avicenna J Med. 2019;9(4):164-8.
1098 48. Al-Tawfiq JA, Kiwan G, Murrar H. Granulicatella elegans native valve infective endocarditis: case
1099 report and review. Diagn Microbiol Infect Dis. 2007;57(4):439-41.
1100 49. Ohara-Nemoto Y, Kishi K, Satho M, Tajika S, Sasaki M, Namioka A, et al. Infective endocarditis
1101 caused by Granulicatella elegans originating in the oral cavity. J Clin Microbiol. 2005;43(3):1405-7.
1102 50. Padmaja K, Lakshmi V, Subramanian S, Neeraja M, Krishna SR, Satish OS. Infective endocarditis
1103 due to Granulicatella adiacens: a case report and review. J Infect Dev Ctries. 2014;8(4):548-50.
1104 51. Patri S, Agrawal Y. Granulicatella elegans endocarditis: a diagnostic and therapeutic challenge.
1105 BMJ Case Rep. 2016;2016.
1106 52. Ramnarain J, Yoon J, Runnegar N. Staphylococcus pasteuri infective endocarditis: A case report.
1107 IDCases. 2019;18:e00656.
1108 53. Mitchell J. Streptococcus mitis: walking the line between commensalism and pathogenesis. Mol
1109 Oral Microbiol. 2011;26(2):89-98.
1110 54. Kim SL, Gordon SM, Shrestha NK. Distribution of streptococcal groups causing infective
1111 endocarditis: a descriptive study. Diagn Microbiol Infect Dis. 2018;91(3):269-72.
1112 55. Boratyn GM, Schaffer AA, Agarwala R, Altschul SF, Lipman DJ, Madden TL. Domain enhanced
1113 lookup time accelerated BLAST. Biol Direct. 2012;7:12.
1114 56. Zheng W, Tan MF, Old LA, Paterson IC, Jakubovics NS, Choo SW. Distinct Biological Potential of
1115 Streptococcus gordonii and Streptococcus sanguinis Revealed by Comparative Genome Analysis. Sci Rep.
1116 2017;7(1):2949.
1117 57. Moschioni M, Pansegrau W, Barocchi MA. Adhesion determinants of the Streptococcus species.
1118 Microb Biotechnol. 2010;3(4):370-88.
1119 58. Elliott D, Harrison E, Handley PS, Ford SK, Jaffray E, Mordan N, et al. Prevalence of Csh-like
1120 fibrillar surface proteins among mitis group oral streptococci. Oral Microbiol Immunol. 2003;18(2):114-
1121 20.
1122 59. McNab R, Forbes H, Handley PS, Loach DM, Tannock GW, Jenkinson HF. Cell wall-anchored CshA
1123 polypeptide (259 kilodaltons) in Streptococcus gordonii forms surface fibrils that confer hydrophobic
1124 and adhesive properties. J Bacteriol. 1999;181(10):3087-95.
1125 60. Connaris H, Crocker PR, Taylor GL. Enhancing the receptor affinity of the sialic acid-binding
1126 domain of Vibrio cholerae sialidase through multivalency. J Biol Chem. 2009;284(11):7339-51.
1127 61. Goulas TK, Goulas AK, Tzortzis G, Gibson GR. Molecular cloning and comparative analysis of four
1128 beta-galactosidase genes from Bifidobacterium bifidum NCIMB41171. Appl Microbiol Biotechnol.
1129 2007;76(6):1365-72.

bioRxiv preprint doi: https://doi.org/10.1101/2020.07.17.206995; this version posted November 14, 2020. The copyright holder for this preprint (which was not certified by peer review) is the author/funder. All rights reserved. No reuse allowed without permission.

62. Chitayat S, Adams JJ, Smith SP. NMR assignment of backbone and side chain resonances for a dockerin-containing C-terminal fragment of the putative mu-toxin from Clostridium perfringens. Biomol NMR Assign. 2007;1(1):13-5.
63. Chitayat S, Adams JJ, Furness HS, Bayer EA, Smith SP. The solution structure of the C-terminal modular pair from Clostridium perfringens mu-toxin reveals a noncellulosomal dockerin module. J Mol Biol. 2008;381(5):1202-12.
64. Fujita K, Oura F, Nagamine N, Katayama T, Hiratake J, Sakata K, et al. Identification and molecular cloning of a novel glycoside hydrolase family of core 1 type O-glycan-specific endo-alpha-N-acetylgalactosaminidase from Bifidobacterium longum. J Biol Chem. 2005;280(45):37415-22.
65. Ashida H, Miyake A, Kiyohara M, Wada J, Yoshida E, Kumagai H, et al. Two distinct alpha-L-fucosidases from Bifidobacterium bifidum are essential for the utilization of fucosylated milk oligosaccharides and glycoconjugates. Glycobiology. 2009;19(9):1010-7.
66. Trastoy B, Lomino JV, Pierce BG, Carter LG, Gunther S, Giddens JP, et al. Crystal structure of Streptococcus pyogenes EndoS, an immunomodulatory endoglycosidase specific for human IgG antibodies. Proc Natl Acad Sci U S A. 2014;111(18):6714-9.
67. Dixon EV, Claridge JK, Harvey DJ, Baruah K, Yu X, Vesiljevic S, et al. Fragments of bacterial endoglycosidase s and immunoglobulin g reveal subdomains of each that contribute to deglycosylation. J Biol Chem. 2014;289(20):13876-89.
68. Cheng AG, Missiakas D, Schneewind O. The giant protein Ebh is a determinant of Staphylococcus aureus cell size and complement resistance. J Bacteriol. 2014;196(5):971-81.
69. Clarke SR, Harris LG, Richards RG, Foster SJ. Analysis of Ebh, a 1.1-megadalton cell wall-associated fibronectin-binding protein of Staphylococcus aureus. Infect Immun. 2002;70(12):6680-7.
70. Tanaka Y, Sakamoto S, Kuroda M, Goda S, Gao YG, Tsumoto K, et al. A helical string of alternately connected three-helix bundles for the cell wall-associated adhesion protein Ebh from Staphylococcus aureus. Structure. 2008;16(3):488-96.
71. Lin IH, Hsu MT, Chang CH. Protein domain repetition is enriched in Streptococcal cell-surface proteins. Genomics. 2012;100(6):370-9.
72. Schroeder K, Jularic M, Horsburgh SM, Hirschhausen N, Neumann C, Bertling A, et al. Molecular characterization of a novel Staphylococcus aureus surface protein (SasC) involved in cell aggregation and biofilm accumulation. PLoS One. 2009;4(10):e7567.
73. Velez MP, Petrova MI, Lebeer S, Verhoeven TL, Claes I, Lambrichts I, et al. Characterization of MabA, a modulator of Lactobacillus rhamnosus GG adhesion and biofilm formation. FEMS Immunol Med Microbiol. 2010;59(3):386-98.
74. Shivshankar P, Sanchez C, Rose LF, Orihuela CJ. The Streptococcus pneumoniae adhesin PsrP binds to Keratin 10 on lung cells. Mol Microbiol. 2009;73(4):663-79.
75. Takahashi Y, Yajima A, Cisar JO, Konishi K. Functional analysis of the Streptococcus gordonii DL1 sialic acid-binding adhesin and its essential role in bacterial binding to platelets. Infect Immun. 2004;72(7):3876-82.
76. Wu H, Zeng M, Fives-Taylor P. The glycan moieties and the N-terminal polypeptide backbone of a fimbria-associated adhesin, Fap1, play distinct roles in the biofilm development of Streptococcus parasanguinis. Infect Immun. 2007;75(5):2181-8.
77. Handley PS, Correia FF, Russell K, Rosan B, DiRienzo JM. Association of a novel high molecular weight, serine-rich protein (SrpA) with fibril-mediated adhesion of the oral biofilm bacterium Streptococcus cristatus. Oral Microbiol Immunol. 2005;20(3):131-40.
78. Seo HS, Xiong YQ, Sullam PM. Role of the serine-rich surface glycoprotein Srr1 of Streptococcus agalactiae in the pathogenesis of infective endocarditis. PLoS One. 2013;8(5):e64204.

bioRxiv preprint doi: https://doi.org/10.1101/2020.07.17.206995; this version posted November 14, 2020. The copyright holder for this preprint (which was not certified by peer review) is the author/funder. All rights reserved. No reuse allowed without permission.

79. Kilian M, Tettelin H. Identification of Virulence-Associated Properties by Comparative Genome Analysis of Streptococcus pneumoniae, S. pseudopneumoniae, S. mitis, Three S. oralis Subspecies, and S. infantis. mBio. 2019;10(5).
80. Reichmann P, Konig A, Linares J, Alcaide F, Tenover FC, McDougal L, et al. A global gene pool for high-level cephalosporin resistance in commensal Streptococcus species and Streptococcus pneumoniae. J Infect Dis. 1997;176(4):1001-12.
81. Granok AB, Parsonage D, Ross RP, Caparon MG. The RofA binding site in Streptococcus pyogenes is utilized in multiple transcriptional pathways. J Bacteriol. 2000;182(6):1529-40.
82. Bishop CJ, Aanensen DM, Jordan GE, Kilian M, Hanage WP, Spratt BG. Assigning strains to bacterial species via the internet. BMC Biol. 2009;7:3.
83. Jensen A, Scholz CFP, Kilian M. Re-evaluation of the taxonomy of the Mitis group of the genus Streptococcus based on whole genome phylogenetic analyses, and proposed reclassification of Streptococcus dentisani as Streptococcus oralis subsp. dentisani comb. nov., Streptococcus tigurinus as Streptococcus oralis subsp. tigurinus comb. nov., and Streptococcus oligofermentans as a later synonym of Streptococcus cristatus. Int J Syst Evol Microbiol. 2016;66(11):4803-20.
84. Tamura K, Stecher G, Peterson D, Filipski A, Kumar S. MEGA6: Molecular Evolutionary Genetics Analysis version 6.0. Mol Biol Evol. 2013;30(12):2725-9.
85. Fujiwara T, Hoshino T, Ooshima T, Sobue S, Hamada S. Purification, characterization, and molecular analysis of the gene encoding glucosyltransferase from Streptococcus oralis. Infect Immun. 2000;68(5):2475-83.
86. Koren S, Walenz BP, Berlin K, Miller JR, Bergman NH, Phillippy AM. Canu: scalable and accurate long-read assembly via adaptive k-mer weighting and repeat separation. Genome Res. 2017;27(5):722-36.
87. Simao FA, Waterhouse RM, Ioannidis P, Kriventseva EV, Zdobnov EM. BUSCO: assessing genome assembly and annotation completeness with single-copy orthologs. Bioinformatics. 2015;31(19):3210-2.
88. Seemann T. Prokka: rapid prokaryotic genome annotation. Bioinformatics. 2014;30(14):2068-9.
89. Almagro Armenteros JJ, Tsirigos KD, Sonderby CK, Petersen TN, Winther O, Brunak S, et al. SignalP 5.0 improves signal peptide predictions using deep neural networks. Nat Biotechnol. 2019;37(4):420-3.
90. Nawrocki EP, Eddy SR. Infernal 1.1: 100-fold faster RNA homology searches. Bioinformatics. 2013;29(22):2933-5.
91. McLaughlin RE, Ferretti JJ. Electrotransformation of Streptococci. Methods Mol Biol. 1995;47:185-93.
92. Alam S, Brailsford SR, Whiley RA, Beighton D. PCR-Based methods for genotyping viridans group streptococci. J Clin Microbiol. 1999;37(9):2772-6.
93. Wiedemann C, Bellstedt P, Gorlach M. CAPITO--a web server-based analysis and plotting tool for circular dichroism data. Bioinformatics. 2013;29(14):1750-7.
94. Rueden CT, Schindelin J, Hiner MC, DeZonia BE, Walter AE, Arena ET, et al. ImageJ2: ImageJ for the next generation of scientific image data. BMC Bioinformatics. 2017;18(1):529.
95. Waterhouse A, Bertoni M, Bienert S, Studer G, Tauriello G, Gumienny R, et al. SWISS-MODEL: homology modelling of protein structures and complexes. Nucleic Acids Res. 2018;46(W1):W296-W303.
96. Madeira F, Park YM, Lee J, Buso N, Gur T, Madhusoodanan N, et al. The EMBL-EBI search and sequence analysis tools APIs in 2019. Nucleic Acids Res. 2019;47(W1):W636-W41.

Figure captions

bioRxiv preprint doi: https://doi.org/10.1101/2020.07.17.206995; this version posted November 14, 2020. The copyright holder for this preprint (which was not certified by peer review) is the author/funder. All rights reserved. No reuse allowed without permission.

Fig 1. Fap1 is not essential for adhesion to sialic acid.

(A) Southern blot of EcoRV-digested gDNA from five different *S. oralis* subsp. *oralis* IE-isolates using a DIG-labeled *fap1* probe. gDNA from *S. oralis* subsp. *oralis* strain ATCC10557 was used as a positive control (+). *fap1* was detected in only two IE-isolates, (B) Adherence of five *S. oralis* subsp. *oralis* IE-isolates to platelets in the presence of 30 μM CBM40 (+). Adherence was expressed as a percentage relative to the same strain in the absence of CBM40 (-). Values are the means for at least three independent experiments, each performed in triplicate, $\pm$ SD. *Statistical significance was tested by two-tailed Student's t-test. *, $P \leq 0.0015$.

Fig 2. β-1,4-linked galactose serves as a receptor for some *S. oralis* subsp. *oralis* isolates.

Binding to β-1,4-linked galactose was tested by the addition of 50 μM CBM71-1.2 following pretreatment with neuraminidase (N^{PRE}) or PBS (-). The graphs show adherence of the $SRRP^-$ (A) and $SRRP^+$ (B) IE-isolates to untreated or neuraminidase-pretreated platelets in presence or absence of CBM71-1.2. Adherence is expressed as a percentage relative to binding of the strains to untreated platelets in the absence of CBM71-1.2. Values are the means for at least three independent experiments, each performed in triplicate, $\pm$ SD. Statistical significance was tested by two-tailed Student's t-test. *, $P \leq 0.015$; NS, not significant.

Fig 3. A Sortase A-dependent surface protein(s) is required for binding of *S. oralis* IE-isolates lacking SRRPs.

bioRxiv preprint doi: https://doi.org/10.1101/2020.07.17.206995; this version posted November 14, 2020. The copyright holder for this preprint (which was not certified by peer review) is the author/funder. All rights reserved. No reuse allowed without permission.

(A) a *srtA* mutant is reduced in binding to platelets. Graphs indicate adherence of IE12 and IE18 *srtA* mutants and complements, with *srtA* or the empty vector (pABG5), relative to parental strains. The contribution of SrtA-dependent surface proteins to β-1,4-linked galactose binding was tested by comparing adhesion to neuraminidase-pretreated platelets (N^{PRE}). (B) Venn diagram showing shared and unique LPxTG-containing proteins in three different *S. oralis* subsp. *oralis* IE-isolates. Comparisons were made by BLASTP, proteins with >80% amino acid identity were considered as shared between strains. (C) As demonstrated by PCR, the presence of IE12_1764 and IE18_0557 correlates with the ability of *fap1*$^{-}$ isolates to bind sialic acid or β-1,4-linked galactose, respectively. *rpoB* was used as a positive control. Adherence data are the means for at least three independent experiments, each performed in triplicate, $\pm$ SD. Statistical significance was tested by two-tailed Student's t-test. *, $P \leq 0.006$.

Fig 4. Csh-like protein is not involved in IE18 binding to β-1,4-linked galactose.

(A) Schematic illustrating the predicted protein architecture of Csh-like from *S. oralis* subsp. *oralis* IE18 (IE18_0557). Csh-like consists of an N-terminal secretion signal (SS), followed by the NR2 domain (PDB: 5L2D), 23 CshA-type fibrils repeats and a cell wall anchoring motif (LPxTG). (B) The non-repeat region of Csh-like (Csh_NRR) is not involved in binding to β-1,4-linked galactose. Unlike CBM71-1.2, the addition of 30 μM of the recombinantly expressed Csh_NRR did not significantly reduce binding of IE18 to neuraminidase-pretreated (N^{PRE}) platelets. Adherence is expressed as a percentage relative to binding of IE18 to neuraminidase-pretreated (N^{PRE}) platelets in the absence of CBM71-1.2 or Csh_NRR. Values are the means for at least three independent

bioRxiv preprint doi: https://doi.org/10.1101/2020.07.17.206995; this version posted November 14, 2020. The copyright holder for this preprint (which was not certified by peer review) is the author/funder. All rights reserved. No reuse allowed without permission.

experiments, each performed in triplicate, ± SD. Statistical significance was tested by two-tailed Student's t-test. *, $P \leq 0.001$; NS, not significant.

Fig 5. AsaA is a novel sialic acid-binding adhesin.

(A) Schematic illustrating the predicted protein architecture of AsaA (IE12_1764) from *S. oralis* subsp. *oralis* IE12. AsaA consists of an N-terminal secretion signal (SS), followed by the non-repeat region predicted to contain a FIVAR/CBM domain and two Siglec-like and Unique domains, followed by 31 DUF1542 domains and a C-terminal LPxTG motif. (B) Comparison of the AsaA Siglec-like and Unique domains tertiary structure, predicted by SWISS-MODEL, to the solved structure of SrpA Siglec-like and Unique domain (5KIQ). (C) An IE12 *asaA* mutant was reduced in binding to platelets. Neuraminidase pretreatment (N^{PRE}) did not further reduced binding of the mutant. (D) Left: schematic illustrating the domains removed in the isogenic IE12 variants. To further evaluate protein production and localization, a 3xFLAG tag (black box) was added to all constructs, including the parental strain (WT-3F). Right: Adhesion of WT-3F and the isogenic AsaA-deletion mutants to platelets. (E) Production of the AsaA deletion variants evaluated by the detection of the 3xFLAG tag in whole-cell lysates by immunodot-blot. (F) Detection of the AsaA-deletion variants on the cell surface by immunofluorescent microscopy. Representative images of Nile red-stained bacteria (red) incubated with anti-FLAG and Alexa Fluor 488-conjugated secondary antibody (green). Bars 1 µm. Adherence is expressed as a percentage relative to binding of the parental strain to untreated platelets. Values are the means for at least three

bioRxiv preprint doi: https://doi.org/10.1101/2020.07.17.206995; this version posted November 14, 2020. The copyright holder for this preprint (which was not certified by peer review) is the author/funder. All rights reserved. No reuse allowed without permission.

1289 independent experiments, each performed in triplicate, ± SD. Statistical significance
1290 was tested by two-tailed Student's t-test. *, P ≤ 0.0004. NS, not significant.
1291
1292 **Fig 6. The Siglec-like and Unique domains of AsaA mediate direct binding to**
1293 **sialic acid on platelets.** (A) Adhesion of IE12 was reduced in a dose-dependent
1294 manner by increasing concentrations of AsaA_NRR. (B) Adhesion of IE12 and the *asaA*
1295 mutant to untreated and neuraminidase pretreated (N^{PRE}) platelets in the presence of 5
1296 µM AsaA_NRR or AsaA_SU_1-2. Adherence is expressed as a percentage relative to
1297 binding of IE12 to untreated platelets in the absence of recombinant proteins. (C) Direct
1298 binding of platelets pretreated with PBS or neuraminidase (N^{PRE}) to immobilized
1299 AsaA_NRR, AsaA_SU_1-2 or GST. A representative image of platelets binding to
1300 immobilized protein is shown. The graph shows the average number of platelets
1301 recovered in three independent experiments performed in triplicate. Statistical
1302 significance was tested by two-tailed Student's t-test. *, P ≤ 0.002. NS, not significant.
1303
1304 **Fig 7. AsaA contributes to *S. oralis* IE12 virulence in a rabbit model of IE.** The two
1305 strains indicated were co-inoculated into six rabbits from two independent experiments
1306 (three rabbits each) performed on different days. Individual values and geometric
1307 means of bacteria recovered from vegetations are shown. Identical symbols indicate
1308 bacteria recovered from the same animal. Log-transformed values were analyzed by
1309 paired Student's t-test. *, P ≤ 0.002.
1310

bioRxiv preprint doi: https://doi.org/10.1101/2020.07.17.206995; this version posted November 14, 2020. The copyright holder for this preprint (which was not certified by peer review) is the author/funder. All rights reserved. No reuse allowed without permission.

Fig 8. AsaA is not required for binding to fibrinogen or fibronectin. The IE12 *asaA* mutant displayed increased binding to immobilized fibronectin, while binding to fibrinogen was not significantly different from that of IE12. Adherence is expressed as a percentage relative to binding of IE12. Values are the means for at least three independent experiments, each performed in triplicate, ± SD. Statistical significance was tested by two-tailed Student's t-test. *, $P \leq 0.02$; NS, not significant.

Fig 9. AsaA can serve as an adhesin in other IE-causing bacterial species. (A) Schematic illustrating the predicted protein architecture of the NRR of AsaA orthologues from *G. haemolysans* M341 (EGF87895.1), *G. elegans* ATCC700633 (EEW93886.2), *S. pasteuri* 915_SPAS (WP_048803571.1) and *S. mitis* B6 (CBJ22549.1). The percentage of amino acid identity to the NRR of AsaA from *S. oralis* subsp. *oralis* IE12 is shown to the right of the schematic. (B) Adhesion to platelets of IE12 and the *asaA* mutant in the presence of 5 µM Gh_AsaA_NRR. Adherence is expressed as a percentage relative to binding of the same strain in the absence of Gh_AsaA_NRR. Values are the means for at least three independent experiments, each performed in triplicate, ± SD. Statistical significance was tested by two-tailed Student's t-test. *, $P \leq 0.0015$; NS, not significant.

Supporting information

S1 Fig. *secA2* distribution parallels that of *fap1* in *S. oralis* subsp. *oralis* IE-isolates. Southern blots of five different *S. oralis* subsp. *oralis* IE-isolates using three different DIG-labeled *secA2* probes amplified from *S. oralis* Uo5, F0392 and

bioRxiv preprint doi: https://doi.org/10.1101/2020.07.17.206995; this version posted November 14, 2020. The copyright holder for this preprint (which was not certified by peer review) is the author/funder. All rights reserved. No reuse allowed without permission.

ATCC6249, each of which represents one of the three distinct *secA2* alleles identified within sequenced *S. oralis* strains. gDNA from the strains used to amplify each probe was used as a positive control for the appropriate blot (+).

S2 Fig. Distribution of genes encoding potential carbohydrate binding adhesins. The presence of the four genes shared between IE12 and IE18 (A) and those unique to IE18 (B) in all five *S. oralis* subsp. *oralis* IE-isolates was determined by PCR. The distribution of these genes was correlated with the ability of the IE-isolates to bind sialic acid and β-1,4-linked galactose. Amplification of *rpoB* was used as a positive control.

S3 Fig. Expression of IE12_1764 and IE18_0557 is *S. oralis* subsp. *oralis*. Expression of IE12_1764 and IE18_0557 in IE12 and IE18, respectively, was analyzed by RT-PCR. In both cases, the expression of *rpoB* served as a positive control. To rule out DNA contamination, cDNA synthesis was performed in the absence of reverse transcriptase (-).

S4 Fig. IE18 *csh-like* mutant forms aggregates. Gram-staining of IE18 and IE18 Δ*csh-like* shows bacterial aggregates that could not be disrupted by vortexing. Representative images captured using a Nikon eclipse Ti inverted microscope with a 40x objective.

S5 Fig. Csh_NRR is properly folded. Representative CD spectra of the recombinantly expressed Csh_NRR at a concentration of 31.3 µM in PBS.

bioRxiv preprint doi: https://doi.org/10.1101/2020.07.17.206995; this version posted November 14, 2020. The copyright holder for this preprint (which was not certified by peer review) is the author/funder. All rights reserved. No reuse allowed without permission.

S6 Fig. An independent IE12 *asaA* mutant is reduced in binding to platelets. Adhesion of an independent IE12 *asaA* mutant to platelets pretreated with neuraminidase (N^{PRE}) or PBS (-). Adherence is expressed as a percentage relative to binding of IE12 to untreated platelets. Values are the means for at least three independent experiments, each performed in triplicate, ± SD. Statistical significance was tested by two-tailed t Student's t-test. *, $P \leq 0.0001$. NS, not significant.

S7 Fig. IE12 *asa*A WT-3F is reduce in binding to platelets.
Adhesion to platelets of a strain expressing AsaA-3xFLAG (WT-3F) is reduced as compared to IE12. However, an *asaA* mutant is further reduced. Adherence is expressed as a percentage relative to binding of IE12. Values are the means for at least three independent experiments, each performed in triplicate, ± SD. Statistical significance was tested by two-tailed Student's t-test. *, $P \leq 0.0007$.

S8 Fig. GST does not reduce binding of IE12 to platelets. Unlike the addition of the recombinantly expressed So_AsaA_NRR (10 µM), the addition of 10 µM of GST alone did not significantly reduce binding of IE12 to platelets. Adherence is expressed as a percentage relative to binding of IE12 in the absence of So_AsaA_NRR or GST. Values are the means for at least three independent experiments, each performed in triplicate, ± SD. Statistical significance was tested by two-tailed Student's t-test. *, $P \leq 0.0001$; NS, not significant.

bioRxiv preprint doi: https://doi.org/10.1101/2020.07.17.206995; this version posted November 14, 2020. The copyright holder for this preprint (which was not certified by peer review) is the author/funder. All rights reserved. No reuse allowed without permission.

S9 Fig. AsaA is not involved in IE18 binding to β 1-4 linked galactose. Adhesion of an IE18 *asaA* mutant to platelets pretreated with neuraminidase (N^{PRE}). Adherence is expressed as a percentage relative to binding of IE18. Values are the means for at least three independent experiments, each performed in triplicate, ± SD. Statistical significance was tested by two-tailed t Student's t-test. NS, not significant.

S1 Table. Prediction of domains within the potential carbohydrate binding proteins. The full amino acid sequence of the putative sialic-acid and β-1,4-linked galactose binding proteins was used to perform BLASTP and Pfam searches.

bioRxiv preprint doi: https://doi.org/10.1101/2020.07.17.206995; this version posted November 14, 2020. The copyright holder for this preprint (which was not certified by peer review) is the author/funder. All rights reserved. No reuse allowed without permission.

Fig 1.

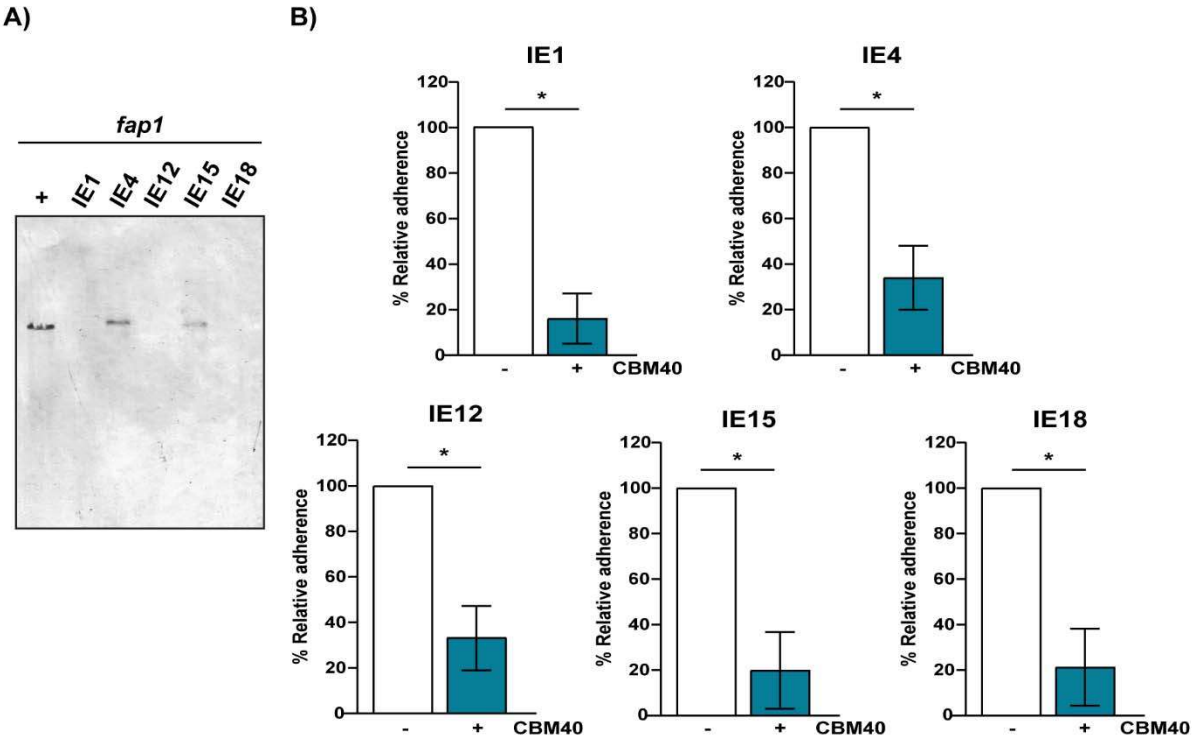

bioRxiv preprint doi: https://doi.org/10.1101/2020.07.17.206995; this version posted November 14, 2020. The copyright holder for this preprint (which was not certified by peer review) is the author/funder. All rights reserved. No reuse allowed without permission.

Fig 2.

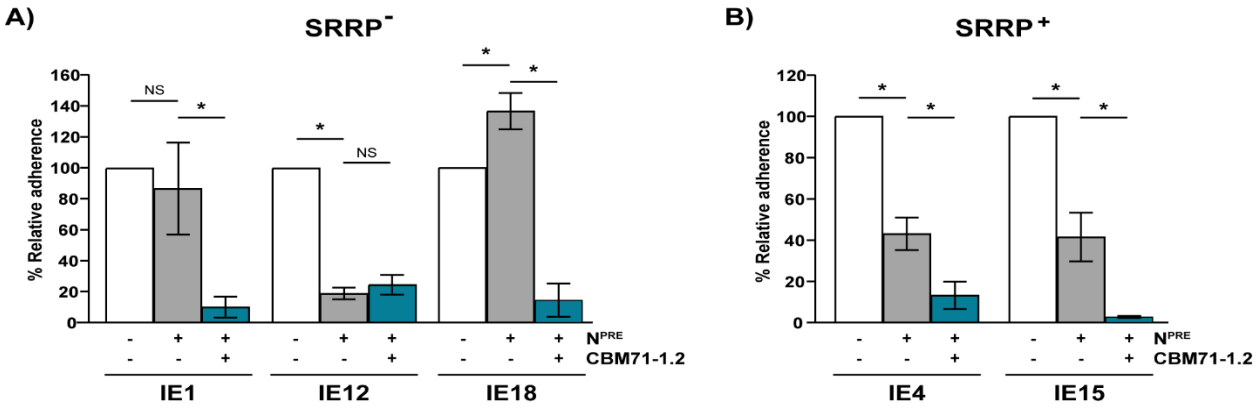

bioRxiv preprint doi: https://doi.org/10.1101/2020.07.17.206995; this version posted November 14, 2020. The copyright holder for this preprint (which was not certified by peer review) is the author/funder. All rights reserved. No reuse allowed without permission.

Fig 3.

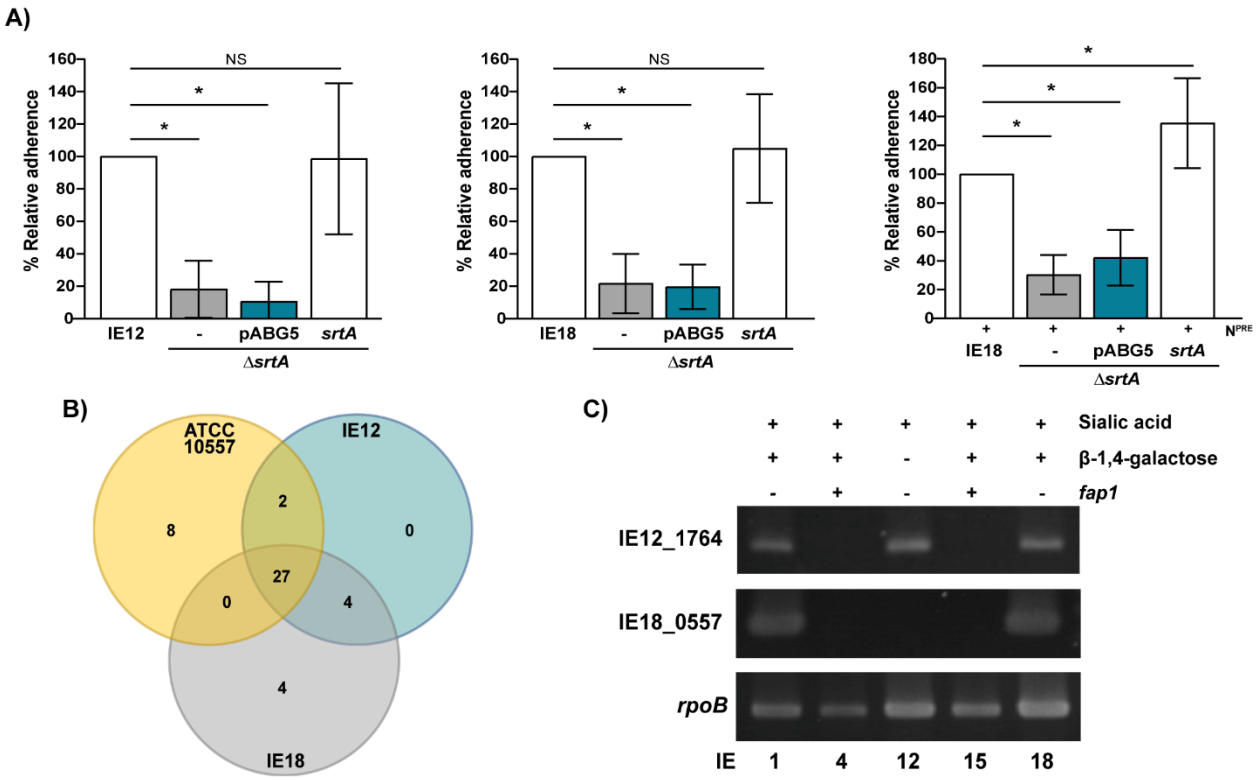

bioRxiv preprint doi: https://doi.org/10.1101/2020.07.17.206995; this version posted November 14, 2020. The copyright holder for this preprint (which was not certified by peer review) is the author/funder. All rights reserved. No reuse allowed without permission.

Fig 4.

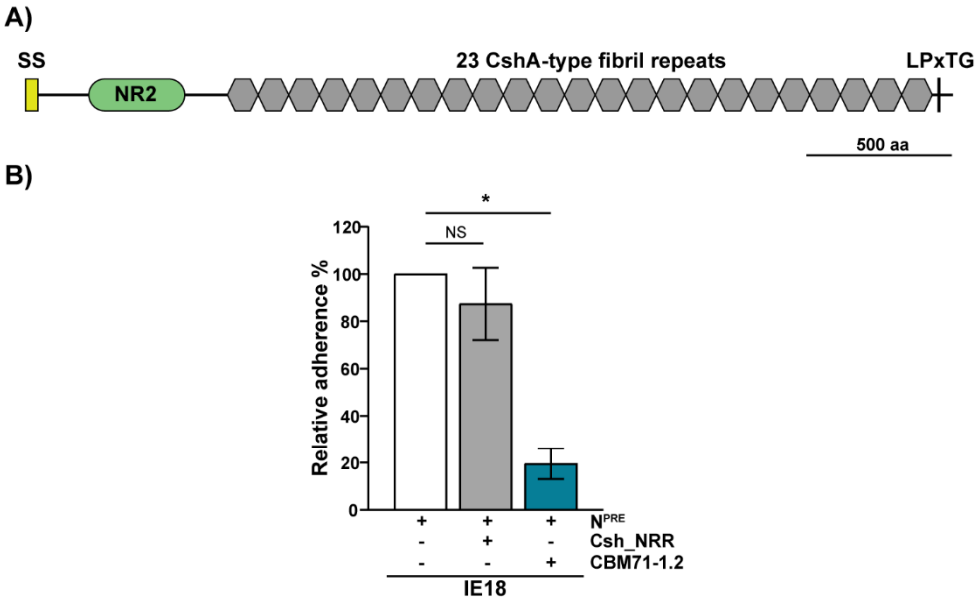

bioRxiv preprint doi: https://doi.org/10.1101/2020.07.17.206995; this version posted November 14, 2020. The copyright holder for this preprint (which was not certified by peer review) is the author/funder. All rights reserved. No reuse allowed without permission.

Fig 5.

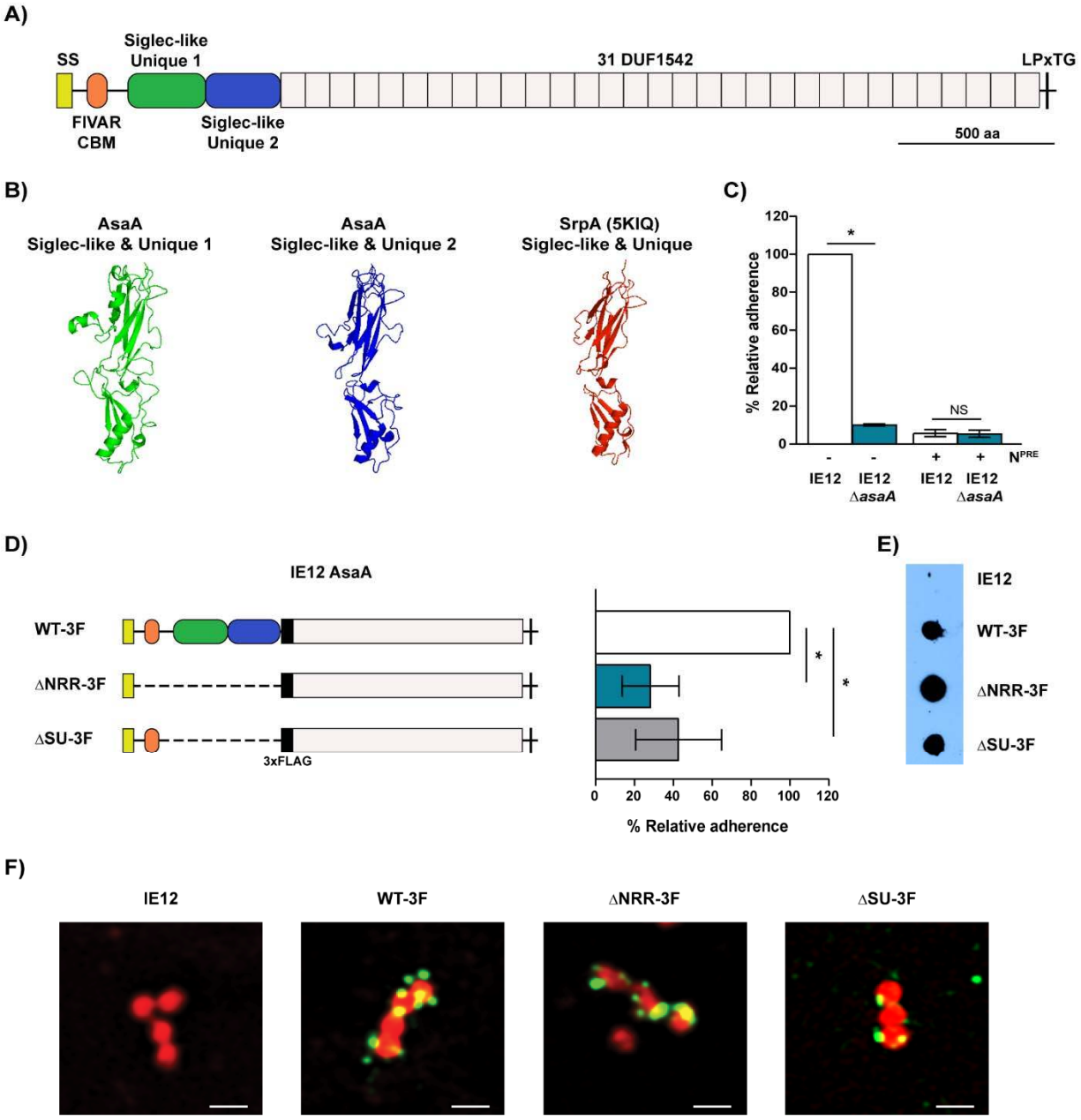

bioRxiv preprint doi: https://doi.org/10.1101/2020.07.17.206995; this version posted November 14, 2020. The copyright holder for this preprint (which was not certified by peer review) is the author/funder. All rights reserved. No reuse allowed without permission.

Fig 6.

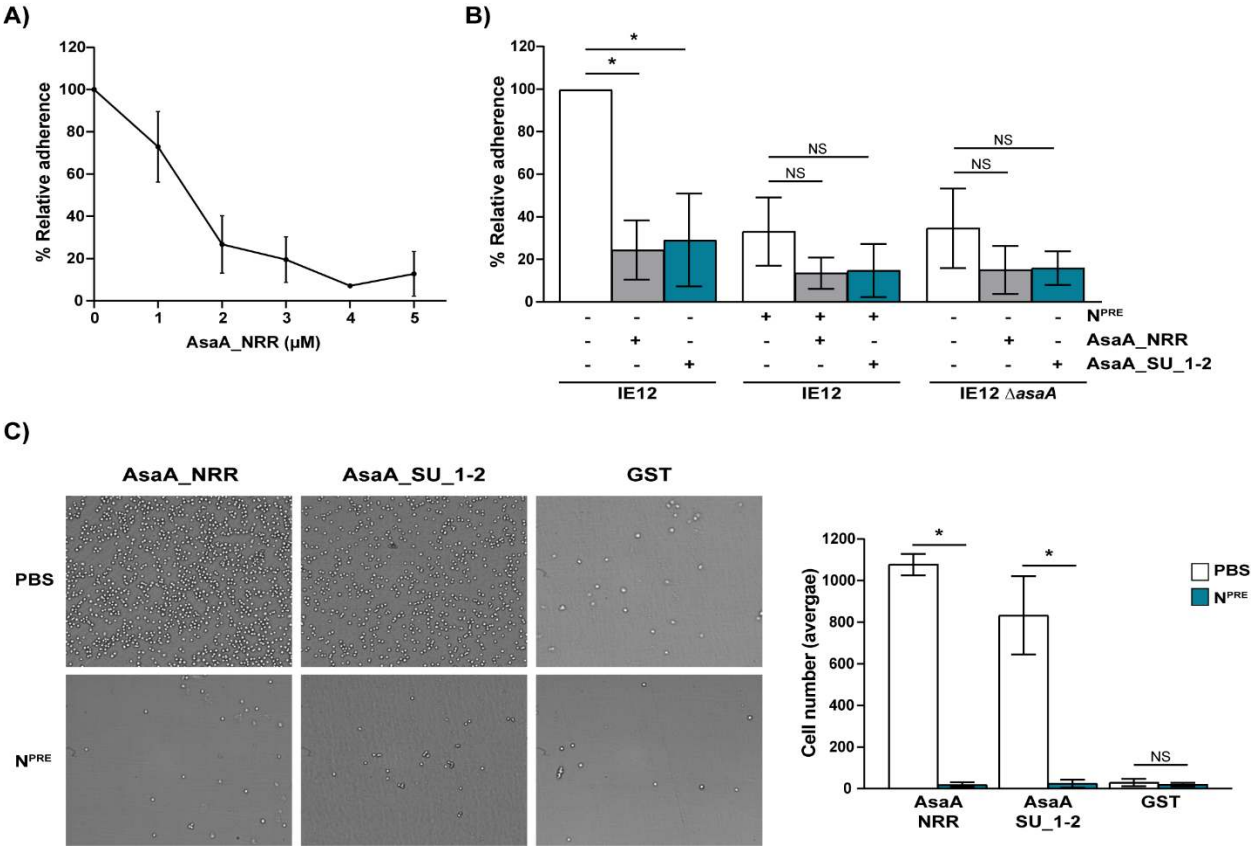

bioRxiv preprint doi: https://doi.org/10.1101/2020.07.17.206995; this version posted November 14, 2020. The copyright holder for this preprint (which was not certified by peer review) is the author/funder. All rights reserved. No reuse allowed without permission.

Fig 7.

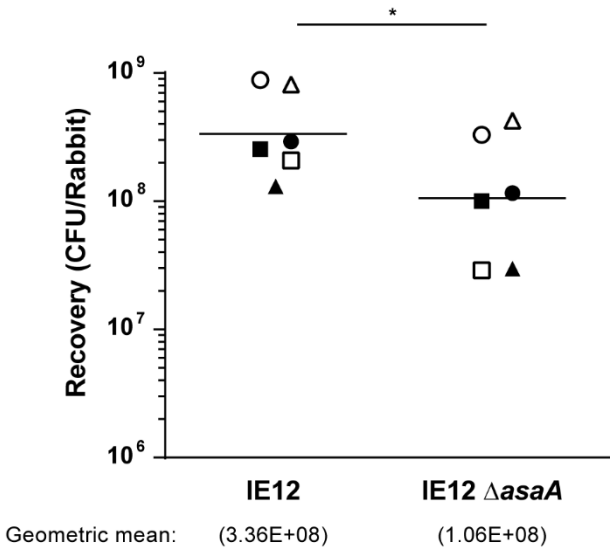

bioRxiv preprint doi: https://doi.org/10.1101/2020.07.17.206995; this version posted November 14, 2020. The copyright holder for this preprint (which was not certified by peer review) is the author/funder. All rights reserved. No reuse allowed without permission.

Fig 8.

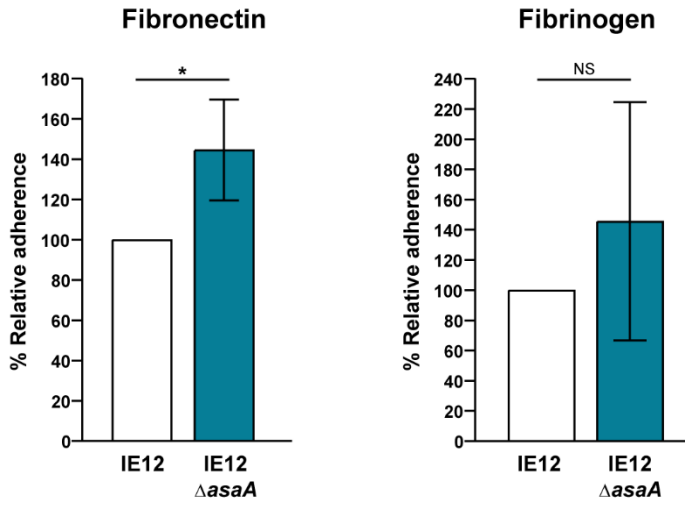

bioRxiv preprint doi: https://doi.org/10.1101/2020.07.17.206995; this version posted November 14, 2020. The copyright holder for this preprint (which was not certified by peer review) is the author/funder. All rights reserved. No reuse allowed without permission.
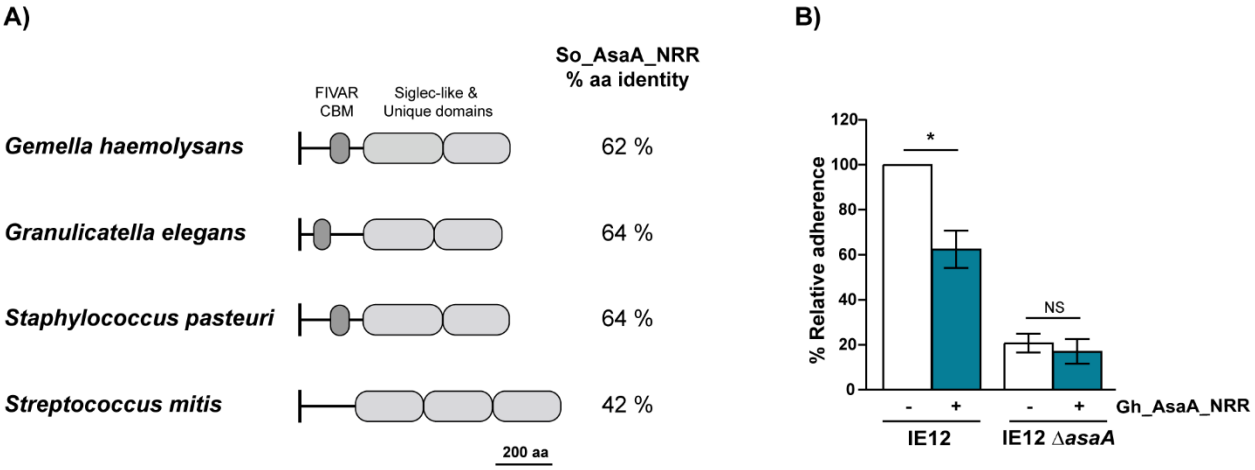
Fig 9.